Journal of Cleaner Production 469 (2024) 143143

Contents lists available at ScienceDirect

Journal of Cleaner Production

journal homepage: www.elsevier.com/locate/jclepro

Techno economic and life cycle assessment of olefin production through CO_2 hydrogenation within the power-to-X concept

Gabriela A. Cuevas-Castillo [a,*], Stavros Michailos [b], Muhammad Akram [a], Kevin Hughes [a], Derek Ingham [a], Mohamed Pourkashanian [a]

[a] Department of Mechanical Engineering, University of Sheffield, 1 Upper Hanover Street, Sheffield, S3 7RA, United Kingdom
[b] School of Engineering, University of Hull, Cottingham Road, Hull, HU6 7RX, United Kingdom

ARTICLE INFO

Handling Editor: Mingzhou Jin

Keywords:
Carbon capture and utilisation (CCU)
Power to olefin
Technoeconomic assessment
Life cycle assessment

ABSTRACT

The paper deals with exhaustive process modelling, techno-economic and life cycle assessment (TEA/LCA) of olefin (ethylene and propylene) production through captured CO_2 and electrolytic hydrogen. Olefins are important building block chemicals with several applications and carbon capture and utilisation (CCU) can provide a sustainable production route. The proposed system involves direct air capture (DAC) of CO_2; proton exchange membrane (PEM) water electrolysis for hydrogen production, methanol synthesis, methanol to olefins (MTO) upgrade, and power generation from off-shore wind turbines. This study proposes a new integrated process as the first attempt to holistically assess a whole CCU assembly aiming at olefins production. Processing modelling has been implemented using the Aspen plus V12.1 and MATLAB R2022a software to solve the mass and energy balances of each unit operation. The modelling results showed a carbon efficiency of 72.3% to ethylene and propylene. In addition, the process is designed and integrated in such a way that no external heat supply is required. A specific energy consumption (SEC) of 150 MJ/kg olefins (41 kWh/kg) has been estimated. A minimum selling price of £3.67 per kg of olefins is required for the proposed process to break-even. The sensitivity analysis has revealed that the major cost driver is the cost of electricity. In addition, the life cycle assessment (LCA) has exposed that the proposed synthesis route of olefins has the potential to reduce the global warming potential (GWP) by 47% compared to fossil - based production. The outcomes of this study can be beneficial to engineering conceptual studies, policy makers and contribute new information to the CCU academic community.

1. Introduction

The use of fossil resources results in an intensive accumulation of greenhouse gases (GHG) that are responsible for the temperature increase of the planet and an increase in temperature above 2 °C will cause an irreversible damage to the planet. In view of this, many have agreed to limit the global temperature increase to 1.5 °C above pre-industrial levels by 2050 according to the Paris Agreement in 2015 (Obrist et al., 2021). This action incorporates decarbonisation strategies and actions for the chemicals, power and fuels industries in the public and the private sectors (Finkbeiner and Bach, 2021). Currently, according to the International Energy Agency (IEA), (2019), the chemical sector globally generates about 1.5 gigaton of CO_2 annually, 27% of which comes from high value chemicals including light olefins and aromatics. The consumption trends in high-income regions are closely related to the rising demand for chemicals; the average amount of plastics consumption in the European Union is between 55 and 80 kg/capita and it is anticipated that the global primary chemicals demand will have increased around 30% by 2030 and up to 60% by 2050 (IEA, 2018). Light olefins, such as ethylene and propylene, are important building blocks of the chemical industry such as plastics, industrial fibres and rubber (Dutta et al., 2019). They are the starting material of the polyethylene and polypropylene packaging which has a 36% global demand (IEA, 2018) and it is predicted to grow by 4% per year by 2025 (GPCA, 2019). This highlights the urgent need to explore sustainable chemical pathways to meet the growing demand for olefins.

Fossil - based olefin production entails the use of high carbon intensive materials such as natural gas, coal and petroleum naphtha that results in augmented GHG emissions (Chung et al., 2023). In recent years, research has been focused on developing and evaluating

* Corresponding author.
E-mail address: gacuevascastillo1@sheffield.ac.uk (G.A. Cuevas-Castillo).

https://doi.org/10.1016/j.jclepro.2024.143143
Received 24 April 2023; Received in revised form 4 June 2024; Accepted 12 July 2024
Available online 14 July 2024

innovative process for a sustainable olefin production. For instance, bio-ethylene can be produced from sugarcane bioethanol dehydration and other crops and it has been implemented at an industrial scale (IEA, 2019). Mohsenzadeh et al. (2017) investigated the techno-economic performance of bio - ethylene production using bioethanol as feedstock. They concluded that the cost of the feedstock has a significant impact on the profitability. Therefore, this approach can only be applied in regions with feedstock availability at competitive prices (Alonso-Fariñas et al., 2018). Alternatively, olefins can be produced using direct CO_2 hydrogenation in one step or via a two-step process with methanol as intermediate in a power to X concept (PtX) coupled with the carbon capture utilisation (CCU) (Zhao et al., 2021). The purpose of the strategy is to utilise CO_2 as a carbon source to produce clean high value-added chemicals such as olefins utilizing renewable H_2 (Kuusela et al., 2021). This concept has also been the subject of several studies. Zhao et al. (2021), explored the economic viability of twenty different olefins manufacturing processes. They compared fossil and renewable processes including the CO_2 to olefin conversion route. They concluded that fossil pathways are more competitive than the renewables routes because of the price of H_2; if the H_2 cost drops by 55% and the plant scale is expanded from 100 to 1000 ktonne per year then costs savings of around 4%–23% can be achieved. Further, Do and Kim (2020), developed a techno economic analysis of green C_2–C_4 hydrocarbon production through CO_2 hydrogenation and renewable H_2. By using solar or wind electricity for hydrogen production, results revealed low net CO_2 emissions but higher hydrocarbon prices ($2.8–5.5 USD/kg C_2–C_4). Nevertheless, when using fossil based options SMR and coal-based hydrogen, results denoted higher emissions (13.6 kg CO_{2e}/kg C_2–C_4) and a cost of $2.6 USD/kg C_2–C_4 product, making the H_2 price the most sensitive factor. Similarly, Savaete (2016) analysed the techno-economic performance of a catalytic CO_2 conversion into olefins using conventional and renewable methanol as an input. The findings revealed that the MTO process using renewable methanol as an input resulted in an ethylene production cost of 3700 €/ton which is higher than the ethylene from conventional methanol, 935 €/ton. It was suggested carbon taxes would need to be high for the MTO feasibility. Pappijn et al. (2020) assessed the economic feasibility and the CO_2 avoidance potential of the electrochemical reduction of CO_2 to ethylene based on a conceptual design excluding the separation and purification stages in the emission counting. They determined that ethylene from electrolytic CO_2 conversion is not feasible under current market conditions and current catalyst performance. They advised the process needs to be powered by green electricity to obtain a net CO_2 balance overall. Regarding environmental analysis, Keller et al. (2020), examined in a cradle to gate evaluation, the environmental impacts of the olefin production using fossil - based and alternative feedstock in Germany. Although it was shown that production using renewable resources reduced GHG emissions, other environmental categories were adversely impacted. Rosental et al. (2020), provided a life cycle assessment of large volume organic chemicals including olefins from CO_2 capture and renewable H_2. Results revealed that the usage of power generated by off-shore wind turbines for CCU methanol, olefins and aromatics synthesis reduces GHG emissions between 88 and 97%. It is important to mention that those reductions included the CO_2 uptake in the capture system. Kuusela et al. (2021) evaluated the greenhouse gas emissions of CO_2 based polypropylene (PP) by applying the power to X concept. While using renewable energy for H_2 production, natural gas and electricity from the grid were consumed in the olefins synthesis, resulting in an estimated gross emission factor of 2.79 kg CO_2e/kg PP. The literature review indicated that there exist some studies that have assessed the economic impact of olefin production, but they have mostly focused on the olefins synthesis and have not included the process modelling of the CO_2 and H_2 feedstock and potential heat integration opportunities between different components. This work includes the simulation of each step in the chain and identifies and applies heat integration. Overall, a holistic LCA and TEA of the whole CCU assembly of a power to the olefins (PtO) pathway is currently missing from the literature and the goal of the present study is to fill this gap.

2. Process description

The plant is located in North Yorkshire, United Kingdom where the Teesside offshore wind farm supplied 546 MW of electricity. The installed capacity (1163 MW) of the wind farm has been calculated by dividing the power consumed (546 MW) in the PtO system with the capacity factor (47%) and then the number of turbines needed for this capacity have been calculated in the System Model Advisor software. Fig. 1 depicts the schematic diagram of the power to olefins process. The PtO produces around 103 ktonne of olefins per year and consists of CO_2 direct air capture (DAC), electrolytic hydrogen production, methanol and olefin synthesis and purification stages in addition to the power generation modelling. Mass and energy balances have been obtained in the Aspen Plus V12.1 and MATLAB R2022a software. Detailed flowsheet models can be found in the Supplementary Information.

2.1. Direct air capture (DAC)

The Carbon Engineering liquid DAC technology has been considered herein and simulations have been conducted based on the data provided in Keith et al. (2018) in which the authors have detailed a description of a direct air capture plant using an aqueous KOH sorbent coupled with a caustic recovery loop to capture almost 1 Mt CO_2/year. This design has been taken as a reference to model the CO_2 capture following the conditions and assumptions of Bianchi (2020) in the Aspen Plus v12.1 software.

Two chemical loops are involved in the atmospheric CO_2 capture. First, an ionic KOH solution with concentrations of 1.0 M OH^-, 0.5 M CO_3^{2-}, and 2.0 M K^+ is used to capture CO_2 forming carbonates. Second, carbonates are precipitated through the reaction of Ca^{2+} to form $CaCO_3$ while Ca^{2+} is replaced by the dissolution of Ca $(OH)_2$. The $CaCO_3$ is calcined to release the CO_2 producing CaO, which is hydrated to regenerate Ca $(OH)_2$. Four major operation units are included and discussed in the following sections as shown in Fig. 2: air contactor, pellet reactor, calciner and slaker (Keith et al., 2018; Sabatino et al., 2021).

2.1.1. Air contactor

The air contactor is simulated in the Aspen plus software as a separator unit in which the CO_2 capture efficiency is fixed to 75% according to the model performed by Keith et al. (2018). The property method is set to the Electrolyte NRTL for the liquid phase and SRK for the gas phase. Initially, the air enters the system where CO_2 reacts with the KOH ionic liquid solution in Eq. (1) to form an aqueous potassium carbonate precipitate. Here, a pressure drop of 0.005 bar occurs (Bianchi, 2020; Keith et al., 2018). Depleted air with low CO_2 concentration is released to the atmosphere while precipitated solution is pumped at 0.005 bar to restore initial pressure for the subsequent steps (Bianchi, 2020; Sanz-Pérez et al., 2016).

$$CO_{2(g)} + 2KOH_{(aq)} \rightarrow K_2CO_{3(aq)} + H_2O_{(l)} \quad (1)$$

2.1.2. Pellet reactor

In the pellet reactor, precipitated solution reacts with calcium oxide to form $CaCO_3$ pellets. The reactor has been modelled as a crystallizer unit available in Aspen Plus. The unit operates at 25 °C and 1 bar. The chemical reaction in Eq. (2) is simulated as a series of equilibrium and dissociation reactions specified in the Aspen properties section and they are described in the Supplementary information. To apply these equations in the crystallizer, the saturation calculation method is selected in the unit specifications. The output of the crystallizer is filtered to recover the $CaCO_3$ that is further sent to the slaker while the liquid solution is recirculated. Part of the calcium leaves the system as fines which are captured in a downstream filter unit (Keith et al., 2018; Sabatino et al.,

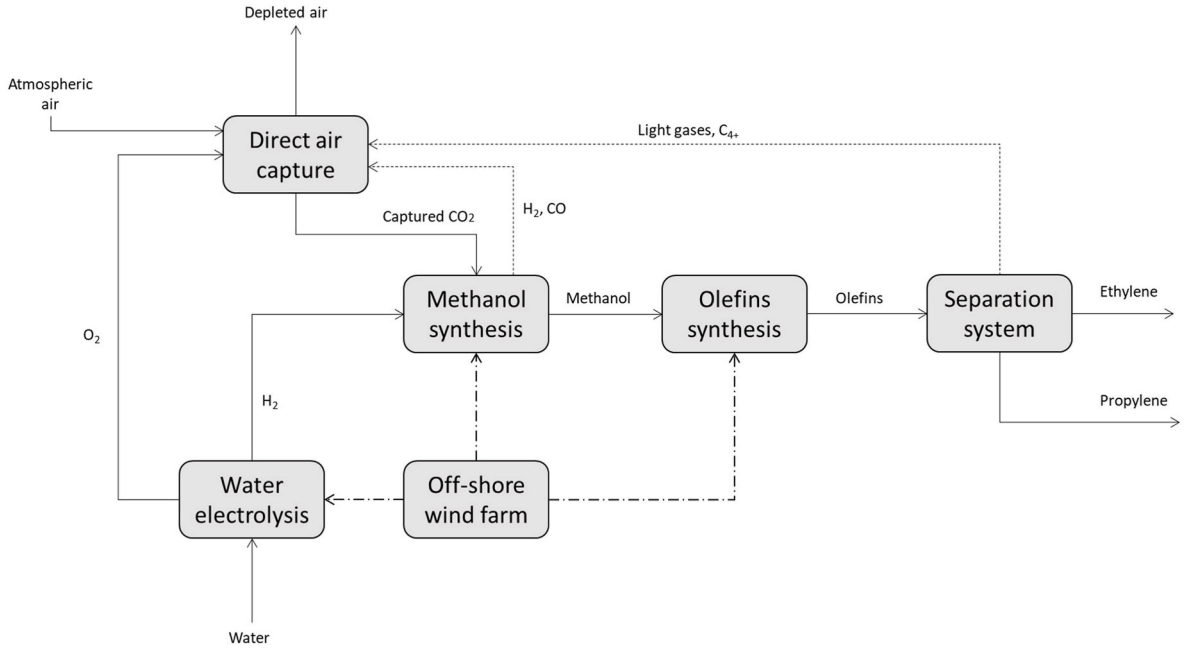

Fig. 1. Schematic diagram of the power to olefin process based on CCU and water electrolysis.

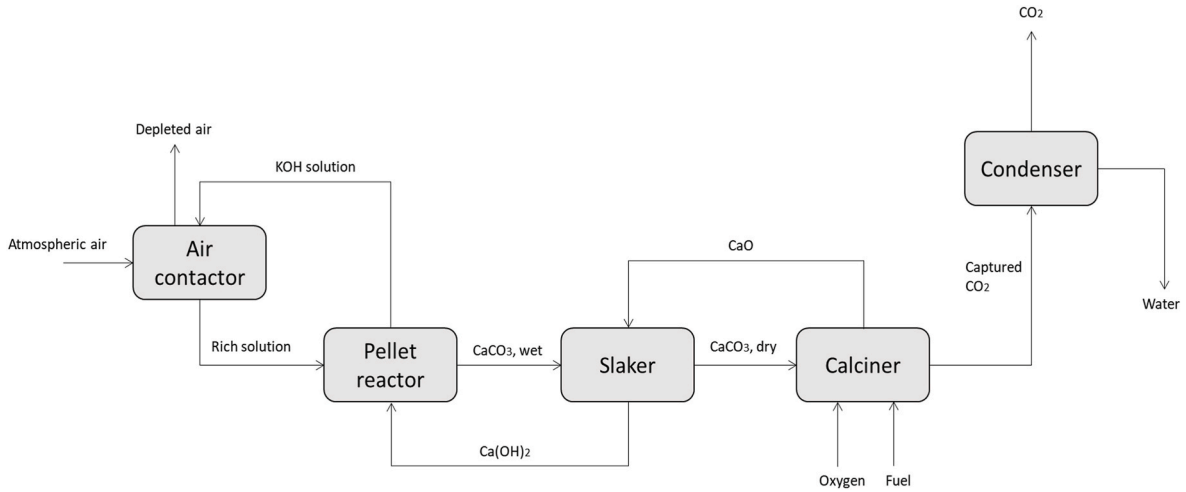

Fig. 2. Block flow diagram of the direct air capture system.

2018; Sanz-Pérez et al., 2016).

$$K_2CO_{3(aq)} + Ca(OH)_{2(s)} \rightarrow 2KOH_{(aq)} + CaCO_{3(s)} \quad (2)$$

2.1.3. Steam slaker

The slaker is modelled for the hydration of quicklime (CaO) and the drying of the $CaCO_3$ pellets. The reactor runs at 85% conversion, 300 °C and atmospheric pressure. Pellets of $CaCO_3$ flows through the reactor to take advantage of the heating provided by the CaO hydration in Eq. (3). At the same time, the water vapour removed from the pellets is used in the hydration as reactant. The operations are simulated as separated units but in a real plant those take place in the same unit. Dried $CaCO_3$ is sent to the calciner for decomposition and the produced Ca $(OH)_2$ is recycled to the pellet reactor. Make up water vapour is injected using steam at 42 bar and 253 °C in a closed loop (Bianchi, 2020; Sabatino et al., 2021).

$$CaO_{(s)} + H_2O_{(l)} \rightarrow Ca(OH)_{2(s)} \quad (3)$$

2.1.4. Calciner

The calcination of $CaCO_3$ occurs through Eq. (4). This is the key step to recover the CO_2 captured by the thermal decomposition of the carbonates which requires a high amount of energy. The calciner is simulated as a conversion reactor working at 900 °C and atmospheric pressure. The conversion efficiency of 98% is set according to Bianchi (2020) and Keith et al. (2018).

$$CaCO_{3(s)} \rightarrow CaO_{(s)} + CO_{2(g)} \quad (4)$$

In the reference of Keith et al. (2018), natural gas is utilised to provide the heat for carbonate decomposition (~5.25 GJ/tonne CO_2). However, in this proposed design, the heat for the calciner is provided by the combustion of the gas streams from the MTO synthesis such as H_2, CO, CH_4, and the heavier olefins C_{4+} (see Fig. 1). Thus, no external fossil resource is employed. Cyclones are added to cool down the products and separate the solid CaO and the CO_2. Finally, water is knocked out and clean CO_2 is sent to a four-stage compressor with intercooling to reach the desired pressure for the methanol synthesis, i.e., 78 bar.

The DAC model utilised herein is based on a pilot plant that captures 1 tonne CO2/day and hence a limitation of the study is that we have assumed similar behaviour of the system for a capture of 0.5 million tonnes per year; nevertheless some of the DAC components such as the air contactor and the pellet reactor are modular and their performance is expected to vary little form the pilot plant. Similar scaling limitations exist with the electrolysis and olefin production sections. To account for these uncertainties we have carried out thorough sensitivity analysis but we acknowledge that more reliable data can be derived from larger scale operations but such data is missing at the moment.

2.2. Renewable hydrogen production

A PEM electrolyser is adopted in this study for the H_2 production. According to Hank et al. (2018), large scales of PEMELs with production capacities >10 Nm^3 H_2/h do offer efficiencies as high as alkaline electrolysers in addition to the high purity of the product at temperatures between 50 and 100 °C. The electrolyser unit has been modelled in Aspen Plus as a stoichiometric reactor operated at 80 °C and 35 bar (Shiva Kumar and Himabindu, 2019). Eq. (5) and Eq. (6) represent the anode and cathode reactions within the reactor. Deionized water is supplied at a flowrate about of 0.01 m^3/kg H_2 (Lundberg, 2019). The lifetime of the equipment is 80,000 h (Shiva Kumar and Himabindu, 2019). Product H_2 is purified by a phase separation unit that removes O_2 from the products stream. Unreacted water and H_2 are cooled down up to 25 °C to facilitate a flash separation of them, and this increases the H_2 purity to 99.99%. The O_2 is split into two streams, one is sent to the oxy-combustion where it will be burnt and the other one is liquefied to produce commercial O_2. Liquefaction is configured in a flash separation and a cryogenic cooling as presented in Johnson et al. (2018). The compression reaches 51 bar and cooling temperature of −123 °C (liquid) followed by expansion to 1.2 bar (Bianchi, 2020).

$$2H^+ + 2e^- \rightarrow H_2 \quad (Cathode) \tag{5}$$

$$H_2O \rightarrow \frac{1}{2}O_2 + 2H^+ + 2e^- \quad (Anode) \tag{6}$$

The electricity consumption of the unit is estimated based on the H_2 HHV and a 75% electrolyser efficiency (Harrison et al., 2014) plus an additional 10% of electricity supplied to cover the demand of the auxiliary equipment (Michailos et al., 2019).

2.3. Methanol synthesis

The following step in the PtO is the catalytic hydrogenation of CO_2 into methanol that acts as the intermediate. The reaction in Eq. (7) takes place at 210 °C and 78 bar in the presence of a commercial catalyst Cu/ZnO/Al_2O_3 according to the conditions of Van-Dal and Bouallou (2013a, b).

$$CO_2 + 3H_2 \leftrightarrow CH_3OH + H_2O \tag{7}$$

Both CO_2 and H_2 should be compressed before entering the reactor. The CO_2 passes through 4 stages compressors to achieve the desired operating pressure (78 bar) and H_2 was compressed from 30 bar to the operating pressure in a one stage compressor. They are heated up to the operation temperature and injected into the fixed bed adiabatic reactor. The device is packed with 44,500 kg of catalyst, assuming CO_2 is the leading source of carbon for the synthesis (Van-Dal and Bouallou, 2013b). The kinetic model used in this paper is taken from Vanden Bussche and Froment (1996) with the adjusted parameters of Mignard and Pritchard (2008). The conditions for the methanol synthesis are presented in Table 1.

After the reaction, the products stream is divided into 2 streams in order to use one of the branches to heat the feed stream. Then, they are mixed again and flashed to separate gases and liquids. The gases are recycled to the compression stage (Pérez-Fortes et al., 2014) whereas the aqueous methanol is sent to the olefins synthesis. Since the olefin reactor performs with a methanol – water mixture, further methanol purification is not required. The kinetic reactions and the simulation model are detailed in the Supplementary Information.

Table 1
Specification for the methanol synthesis (Van-Dal and Bouallou, 2013b).

Parameter	Value	Unit
Reactor type	Fixed bed adiabatic	–
Operating temperature	210	°C
Operating pressure	78	bar
Catalyst density	1775	kg/m^3
Catalyst bed porosity	0.4	–

2.4. Olefin synthesis and separation

The olefin synthesis is modelled as a set of parallel reactions (Fig. 3) based on the work conducted by Lu et al. (2016). The products of the olefins reactor are CH_4 (methane), C_2H_4 (ethylene), C_3H_6 (propylene), C_3H_8 (propane), C_4 (butene) and C_5 (pentene). Also coke formation is taken into account as part of the reaction set. The reactor is simulated as a continuous stirred tank reactor (CSTR) using a commercial SAPO-34 catalyst at a temperature of 465 °C and at atmospheric pressure as proposed in Lu et al. (2016). After use, the catalyst is sent to a regenerator unit where deposited coke is burned and the catalyst is regenerated. The cost of the regenerator unit is included in the purchased equipment cost of the synthesis reactor. Similarly, regarding the environmental performance, the emissions generated by the catalyst regenerator, are considered negligible compared to the total plant emissions. Additionally, the energy recovered from coke burning is minimal compared to the overall energy needs of the plant, therefore, it was excluded from the energy integration.

The kinetic reaction rate of each component is a function of the methanol concentration and the coke deactivation function The kinetic

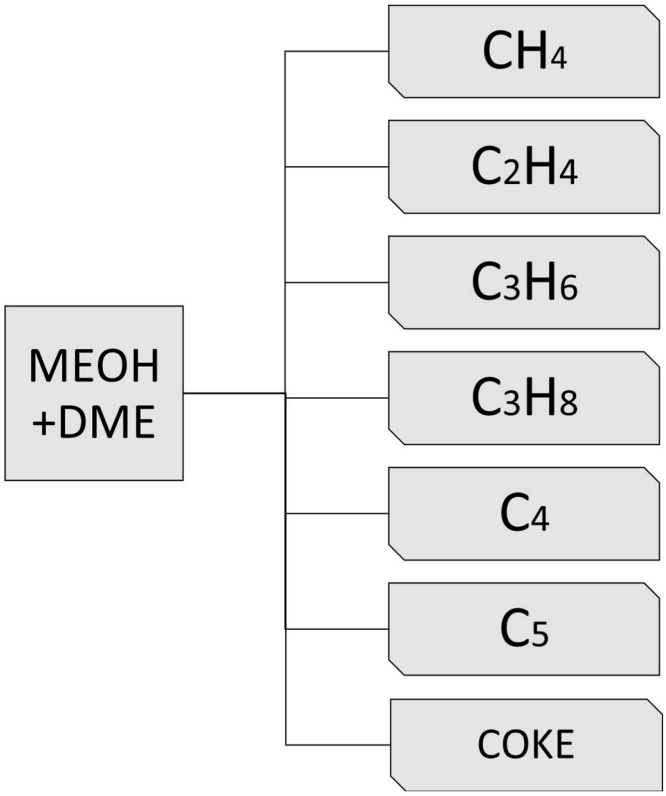

Fig. 3. MTO reactions schematic taken from Lu et al. (2016).

model has been applied in MATLAB and solved using the non-linear system solver *fsolve* and the results were transferred to Aspen Plus by employing a user model unit operation using as intermediate Microsoft Excel (Fontalvo, 2014). Thus, the user model in Aspen Plus was used as a black box and the flowrates of the outputs were specified in the MATLAB module. A detailed flowsheet, the kinetic constants and the set of equations involved in MATLAB can be found in the Supplementary information.

After synthesis, the olefins need to be purified through a sequence of distillation columns (Fig. 4) in order to increase their purity to a chemical grade (>95%). The purification section follows the conditions of Salkuyeh and Adams (2015). The unreacted methanol, water, and the olefins leaving the reactor are cooled to 60 °C and flashed to separate liquid water and methanol from gaseous olefins. The gaseous stream is compressed to 35 bar, cooled up to 40 °C and flashed to remove the remaining water and methanol before entering the columns sequence. For the compressors and gas turbines, the mechanical and isentropic efficiencies are set to be 95% and 90%, respectively (Michailos et al., 2019). During the cooling, heat is recovered to generate low pressure steam that supplies heat for the columns reboiler. Dehydrated olefin are sent to the de - ethanizer (1), here, the ethylene and the other lighter gases (CH_4, CO and remaining CO_2) are separated from the propylene and the heavier components at pressure of 35 bar. Then, the ethylene and light gases are sent to the de - methanizer (2) where light gases are separated from the ethylene at 34 bar. Ethylene is purified in the C_2 splitter (3) that runs at 10 bar where it achieves high purity. Propylene and heavier olefins from the de - ethanizer are move to the de - propanizer (4) where the propylene and propane are recovered at the top of the column and the heavier C_4 and C_5 olefin at the bottoms (Yang and You, 2017). The propylene and propane have a close boiling point; therefore, the desired purity of propylene is achieved by employing a C_3 splitter (5).

Propylene and propane can be used as refrigerants in the column's condensers. Hence, propylene is used in the C_2 splitter to supply part of the cooling duty at −52 °C; similarly, propane is employed in the de - ethanizer condenser at −17 °C, both modelled as open refrigerant cycles. In addition to this, the external refrigerant utility is used to supplement the cooling requirements in all the columns. Further details of the operating conditions of the columns sequence and the refrigerant cycle can be consulted in the Supplementary information.

2.5. Electricity supply

2.5.1. Off-shore wind farm electricity supply

A dedicated off-shore wind farm close to the plant was considered to provide the electricity and the wind farm is located in Teesside UK. Modelling the wind turbines requires the wind speed profile of the specific location to estimate the power generation. To perform this, the System Advisor Model (SAM) software is used. SAM uses the wind profile, a commercial turbine model and the nameplate capacity of the farm to estimate the hourly power output. The wind profile is obtained by providing the location coordinates in the software Metereonorm v7.2 and subsequently the temperature, pressure, wind speed and direction are provided as outputs (Meteotest, 2020). It is important to mention

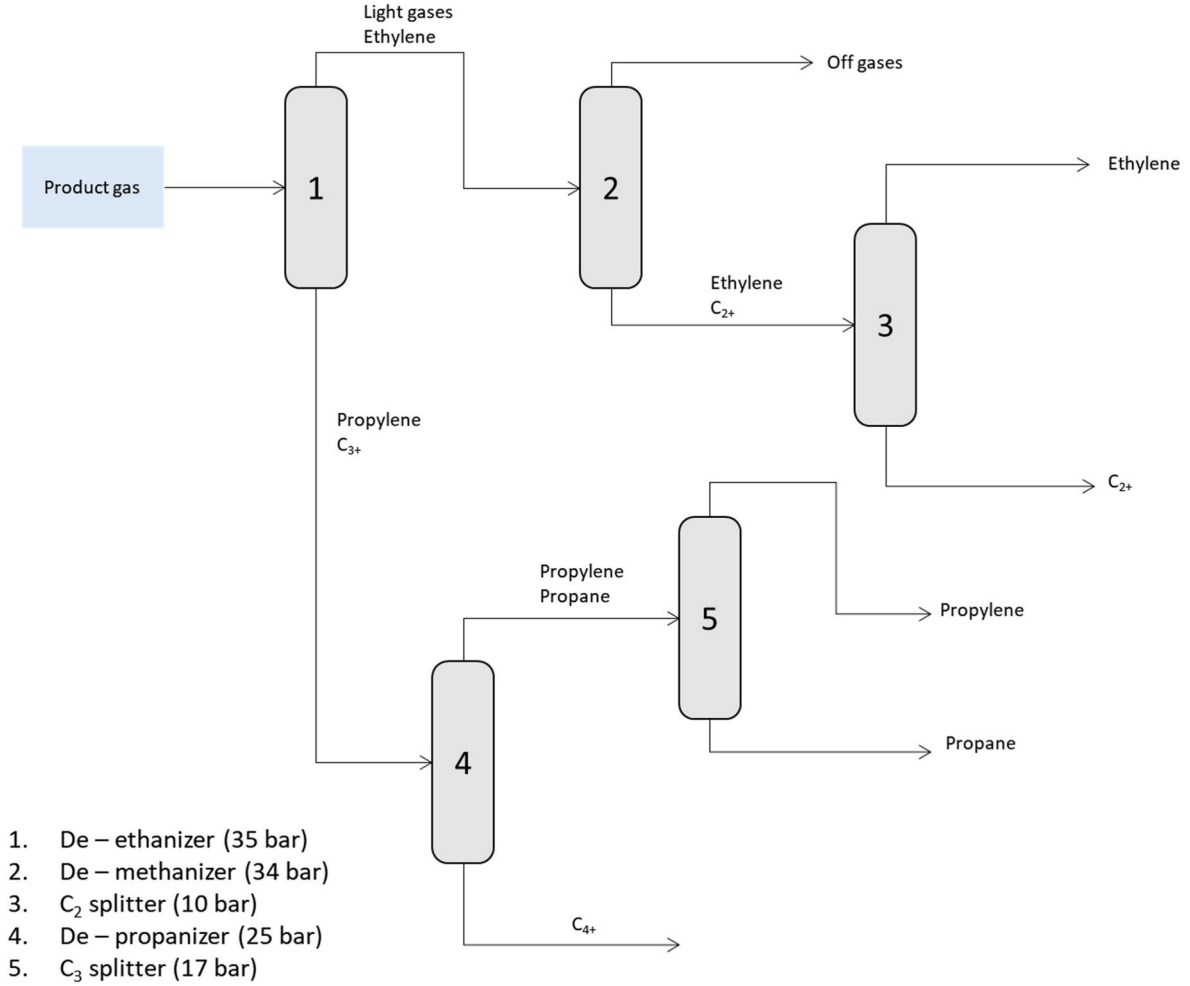

Fig. 4. Process flow diagram of the olefins separation.

that the measures of wind speed are provided at a default height of 10 m while the commercial turbine model chosen is the Senvion 6.2M126 off-shore with a turbine height of 80 m. Therefore, the adjusted wind speed at the actual height is calculated using Eqs. (8) and (9) (Manwell et al., 2010).

$$\alpha = \frac{0.37 - 0.088\ ln\ (U_{ref})}{1 - 0.088\ ln\left(\frac{z_{ref}}{10}\right)} \tag{8}$$

$$\frac{U(z)}{U(z_{ref})} = \left(\frac{z}{z_{ref}}\right)^{\alpha} \tag{9}$$

Where:

α is the power law exponent
U_{ref} is the wind speed at the reference height
$U(z)$ is the wind speed at the current height
z is the actual height
Z_{ref} is the reference height

The SAM software gives an estimation of the real power output provided by the wind farm; however, the plant requires energy continuously without any fluctuations. For that reason, a backup energy strategy is proposed to have a constant power supply. This strategy consists of utilizing the grid network as a storage system when excess of electricity is produced while retrieving electricity from the grid when there is insufficient power generation. The wind farm has been sized in such a way that the electricity sent to and retrieved from the grid is in balance. In addition, the network cost of using the grid is added to the economic analysis. In addition, the wind profile and hourly power output are available in the Supplementary information.

2.5.2. Organic Rankine cycle

A heat integration is implemented in the whole PtO process. The maximum temperature difference between the hot and cold streams is fixed in 10 °C. Cooling duty for the electrolyser and the MTO is provided by cooling water (CW) that after being used, is sent to an Organic Rankine cycle (ORC) for electricity generation (Fig. 5). In the ORC, R245Fa is pumped at 3 bar towards the evaporator and absorbs heat from the water that enters at 79 °C and leaves at 41 °C. A turbine unit recovers the energy as electricity due to the expansion of the vapour. After that, the saturated fluid vapour is condensed to return at the initial conditions. The system is modelled in a closed loop and 5% of the cooling water lost because of evaporation is counted (Van-Dal and Bouallou, 2013a).

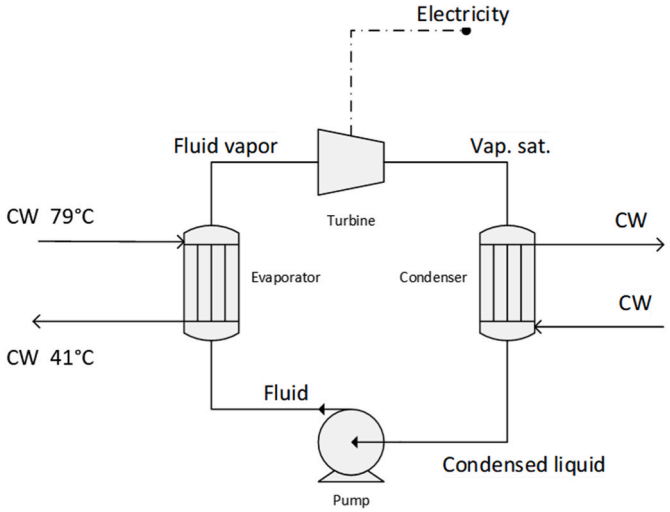

Fig. 5. Organic Rankine Cycle.

3. Key performance indicators

3.1. Technical performance indicators

The performance of the PtO process is assessed in technical, economic, and environmental perspectives. Carbon efficiency (C_e), specific energy consumption (*SEC*) and additional indicators such as overall CO_2 conversion and CO_2 to olefin ratio are included in the technical performance. Economic and environmental performance indicators are described in the subsequent sections.

The carbon efficiency determines the fraction of the original carbon source that is found in the products as part of the conversion. Eq. (10) correlates the moles of carbon in the olefin products (ethylene and propylene) and the moles of carbon present in the CO_2 feedstock (Arnaiz del Pozo et al., 2022).

$$C_e = \frac{\dot{n}_{Cethylene} + \dot{n}_{Cpropylene}}{\dot{n}_{CCO_2}} \tag{10}$$

The specific energy consumption (*SEC*) is defined as the energy requirement per unit mass of the product, Eq. (11).

$$SEC = \frac{Energy\ consumption\ [MW]}{Mass\ flowrate\ of\ products\ \left[\frac{kg}{s}\right]} \tag{11}$$

Similarly, complementary indicators include the amount of CO_2 required per tonne of olefins output (kg/kg) and the overall CO_2 to the olefin conversion denoted in Eq. (12):

$$Overall\ CO_2\ conversion = \left(\frac{\dot{n}_{CO2-input} - \dot{n}_{CO2-output}}{\dot{n}_{CO2-input}}\right) \times 100 \tag{12}$$

Where $n_{CO2\text{-}input}$ is the moles of CO_2 that enters the system, and. $n_{CO2\text{-}output}$ is the moles of CO_2 that are released to the atmosphere during the capture and synthesis.

3.2. Economic analysis

The economic assessment of the PtO plant was completed by applying a typical discounted cash flow analysis to estimate the olefin minimum selling price (MSP) in £/kg. This method requires the calculation of the total capital and operating expenditures (CAPEX/OPEX). The lifetime of the project is 20 years and the plant operates 8000 h per year Table 2.

Estimation of CAPEX requires the purchased equipment cost (PEC) calculation. The equipment costs have been taken from relevant literature and adjusted to the current size using the scaling factor method, Eq. (13).

$$C = C_0\left(S/S_0\right)^{f} \tag{13}$$

Where f is the scaling factor, C and S are the actual equipment cost and size, respectively. C_0 and S_0 are the base cost and size of the unit in the reference. Equipment cost data are detailed in the Supplementary information. For the DAC equipment, there is no agreement of the scaling

Table 2
Main assumptions for the economic evaluation.

Parameter	Units	Value
Plant location	–	United Kingdom
Base year	–	2021
Annual production	ktonne/y	103
Lifetime of the project	years	20
Discount rate	%	10
Depreciation method		straight line
Operating hours	h/y	8000

factor used since the technology is under current research. However, according to Keith et al. (2018), the air contactor and pellet reactor are modular units and their capital cost per unit capacity is almost constant down to 100 ktonne CO_2/year, therefore, a factor of 1 is used in Eq. (13). On the other hand, calciner and slaker costs strongly depend on size and several studies (Fasihi et al., 2019; McQueen et al., 2020; Mostafa et al., 2022; Peters et al., 2019; Prats-Salvado et al., 2022; Sabatino et al., 2021) suggest an exponent of 0.7 as a conservative value.

The Chemical Engineering Plant Cost Index (CEPCI) was utilised to convert the cost plant equipment from the reference base year to the current year. When the cost of the equipment is reported in a different currency than GBP, the value is converted to the current GBP by the exchange rate for the year of reference and then updated to the actual year. In the electrolyser, an extra 28% cost for auxiliaries has been accounted for the PEC as suggested by Buttler and Spliethoff (2018).

The Lang factor methodology is applied to the PEC to determine fixed capital investment (FCI), total direct cost (TDC) and indirect costs (IDC). The factors for installation, instrumentation and controls, piping, electrical systems, buildings, yard improvements, and land are given in Table 3.

The OPEX include variable and fixed operating costs. The variable costs, comprising raw materials, process water, catalyst, and disposals are calculated based on their market prices and simulation results. The catalysts are accounted for a renewal of two years and the levelized cost of electricity (LCOE) has been calculated by the SAM software. Fixed operating costs, supervision, maintenance, insurance, and general plant overhead are computed using default factors as specific percentages of the PEC. In addition, variable and fixed costs are summarized in Table 4.

Labour is estimated using the empirical Eq. (14) proposed by Peters and Timmerhaus (2002).

$$h_{labour}\left[\frac{h}{year}\right] = 2.13 \times plant\_capacity\left[\frac{kg_{output}}{h}\right]^{0.242} \times n_{process\_steps} \times \frac{h_{plant\_operation}}{24} \quad (14)$$

Plant capacity refers to the hourly production of olefin in kg/h, *n process steps* is the number of subsections that significant physical or chemical changes are carried out and the *h plant hours* represents the total working hours per year. The labour rate is taken at £15/h according to the Office for National employment statistics (Office for National Statistics, 2020).

The minimum olefin price is the break-even point at which NPV is equal to zero, Eq. (15).

Table 3
CAPEX estimation methodology (Fernanda Rojas Michaga et al., 2022; G. Towler and R. Sinnott, 2008).

Component	Lang factor
Purchased Equipment Cost (PEC)	1
Installed direct costs (IDC)	PEC + (1) + (2) + (3) + (4)
(1) Purchased equipment installation	0.39*PEC
(2) Instrumentation and controls	0.26*PEC
(3) Piping	0.31*PEC
(4) Electrical systems	0.1*PEC
Non-installed direct costs (NIDC)	(5) + (6) + (7)
(5) Buildings	0.29*PEC
(6) Yard improvements	0.12*PEC
(7) Land	0.06*PEC
Total direct costs (TDC)	(ICD) + (NIDC)
Indirect costs (IDC)	0.255*PEC
Fixed Capital Investment (FCI)	TDC + IDC
Start-up costs	0.05*FCI
Interest during construction	Estimated
Working Capital (WC)	0.05*FCI
CAPEX	FCI + Start-up costs + interest during construction

Table 4
Variable and fixed costs.

Fixed operating and maintenance costs (O&M) (Fernanda Rojas Michaga et al., 2022; Herz et al., 2021)	Basis	Factor	
Operating Labour (OL)	Eq. 14	–	–
Operating Supervision (OS)	OL	0.25	–
Direct overhead (DO)	OL + OS	0.5	–
General overhead	OL + OS + DO	0.5	–
Maintenance labour	FCI	0.015	–
Maintenance materials	FCI	0.015	–
Insurance and tax	FCI	0.01	–
Financing working capital	WC	0.1	–
Variable costs	*Unit*	*Value*	*Reference*
Catalyst price (MeOH)	£/kg	93.2	Pérez-Fortes et al. (2016)
Catalyst price (MTO)	£/kg	81.8	Knighton et al. (2020)
Electricity wind	£/kWh	0.051	SAM software
Electricity grid[a]	£/kwh	0.025	Eurostat (2021)
Wastewater treatment	£/tonne	0.42	Peters and Timmerhaus (2002)
Cooling water	£/tonne	0.03	Peters and Timmerhaus (2002)
Process water	£/m^3	0.08	Keith et al. (2018)
Ca disposal and make up	£/tonne CO_2	0.16	Keith et al. (2018)

[a] Only the cost for the use of the network is computed.

$$NPV = \sum_{n=1}^{20}\left(\frac{Cash\ flow}{(1+i)^n}\right) = 0 \quad (15)$$

Further, a sensitivity analysis is conducted to analyse the effects of the key parameters over the olefin MSP applying a change of ±25% to the original values. The parameters of interest are the LCOE, the electrolyser investment cost, the IRR, the O_2 price, and the CO_2 capture cost expressed as the levelized cost of CO_2 ($LCCO_2$). The $LCCO_2$ is the sum of the levelized capital cost (LCC) of the DAC, the DAC operation and maintenance (O&M) cost and the energy cost required for the CO_2 capture. The $LCCO_2$ and LCC of the capture system are estimated using Eq. (16) and Eq. (17) found in the reference of Keith et al. (2018).

$$LCCO_2 = LCC + DAC\ O\&M + energy\ cost \quad (16)$$

$$LCC = C_i \times \frac{CRF}{U} \quad (17)$$

Where: C_i is the capital cost intensity per unit capacity (U), calculated by applying a Lang factor of 3.2 to the DAC equipment cost, and CRF is the capital recovery factor detailed in Eq. (18).

$$CRF = \frac{i \times (1+i)^n}{(1+i)^n - 1} \quad (18)$$

Where i is the discount rate and n is the number of years for the project. Finally, DAC *O&M* are taken as $42/tonne-$CO_2$ (Keith et al., 2018).The energy cost was neglected since the energy input in the CO_2 capture is supplied by internal resources.

3.3. Environmental assessment

Life Cycle Assessment (LCA) has been applied to determine the environmental impacts of the proposed PtO infrastructure. The environmental impact of turning the CO_2 captured into an olefin product was assessed over the ten baseline impact categories employing CML 2 baseline 2000 impact method. A *cradle to the gate* approach has been

utilised and hence the distribution, use and final disposal are not included (Alonso-Fariñas et al., 2018; Jiang et al., 2019; Rosental et al., 2020; Xiang et al., 2015). This approach has been adopted as products properties, utilisation and disposal are (or can be) identical for the CO_2-based and fossil - based olefins. The framework of this analysis follows the standardized methodology of ISO 14040 in which four steps are involved: goal and scope, inventory data collection, impact categories, and interpretation of results (Xiang et al., 2015). The model was developed in Simapro software v9.4.0.2.

3.3.1. Goal and scope

The goal of the current LCA is to quantify the global warming potential (GWP) of the olefin production using carbon capture utilisation and the power to X approach. Other categories such as abiotic depletion, eutrophication, and ozone depletion are also considered and reported in the Supplementary information.

3.3.2. System boundaries

Fig. 6 illustrates the system boundaries that include the relevant process steps from *cradle to gate*. The LCA includes all material and energy inputs as well as the emissions to the water, soil, and air involved in the processing. The life cycle steps of CO_2 capture, H_2 production through water electrolysis, olefin synthesis and separation in addition to the wind electricity supply are considered. The CO_2 captured (uptake) is not accounted for as negative emissions since at the product end of life, it is released as positive emissions adding up to zero in a carbon neutrality cycle (Rosental et al., 2020). Infrastructure for the DAC, olefin synthesis and electrolyser are not considered due to their low contribution to the environmental impacts (Lundberg, 2019). However, infrastructure emissions of the off-shore wind farm were taken into account.

3.3.3. Functional unit and allocation method

The functional unit is defined as 1 kg of olefin (in our case summation of ethylene and propylene), since butene and pentene are on-site utilised to run the DAC calciner, and therefore no outputs are reported for them. Despite O_2 is considered as unintended product, it is considered in the emissions counting. According to the ISO-14044 guidance, the first step is to avoid or minimise allocation wherever it is possible by subdividing the system into two or more sub processes (Ekvall and Tillman, 1997). Olefin and commercial O_2 are the products of the PtO. The strategy to avoid an allocation between these two different products, is the subdivision of the water electrolysis from the rest of the plant (Fig. 6). Thus, an exergy analysis is applied to allocate water electrolysis emissions between H_2 and O_2 and then, the resulting allocated emissions to H_2 are used to calculate the overall process impacts.

3.3.4. Data collection and impact assessment

The life cycle inventory (LCI) for the DAC, electrolysis and MTO synthesis and separation is constructed from the mass and energy balances obtained from the process modelling results, relevant literature, and using the datasets available in the Ecoinvent database v3.1 (Garcia-Garcia et al., 2021; Kibria Nabil et al., 2021; Liu et al., 2020a; Rosental et al., 2020). The catalyst LCA impact is typically neglected (Althaus et al., 2007) and this approach has been followed herein. The complete LCI is found in the Supplementary information.

The impact categories studied are the Global Warming Potential (GWP), abiotic depletion potential (ADP), eutrophication (EP) and ozone layer depletion (ODP). However, only the GWP is presented, compared, and discussed. The other impact categories are studied in this analysis as they represent the commonly affected environmental impacts (Garcia-Garcia et al., 2021) but they can be found in the Supplementary information.

4. Results and discussion

4.1. Process modelling results

The process flow diagram for the proposed power to olefins process, is illustrated in Fig. 7.

The designed plant has a production rate of 103.4 ktonne/y of olefins. For that purpose, around 876,600 ktonne/y of air at 400 ppm CO_2 concentration (stream 1) was injected to the DAC producing 505.2 ktonne/y of captured CO_2 (stream 3) and releasing depleted air to the atmosphere at 100 ppm CO_2 concentration (stream 2). Additionally, 708 ktonne/y of water (stream 4) were required to produce 76 ktonne/y of H_2 (stream 7) and 598 ktonne/y of O_2. In the latter, around 67% of the stream was liquefied to be sold as a co-product (stream 5) while the remaining was sent to the DAC for oxy-combustion (stream 6). The H_2 along with the captured CO_2 were sent to the methanol synthesis. After the reaction, the outlet stream (stream 8) was cooled down and flashed to separate gases from the MeOH/H_2O liquid mixture. The cooled gases are recycled to the reactor (stream 9) and a purge with most of the unreacted H_2 was sent to the DAC for combustion (stream 10). The MEOH/H_2O mixture (stream 11) is converted into olefins in the olefin

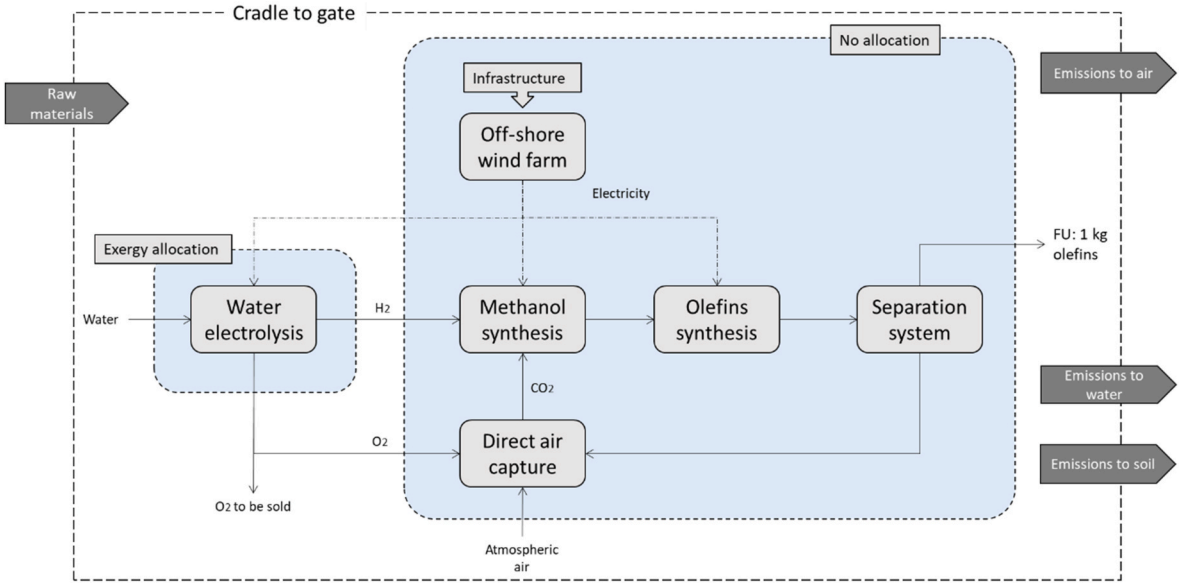

Fig. 6. System boundary for the PtO process.

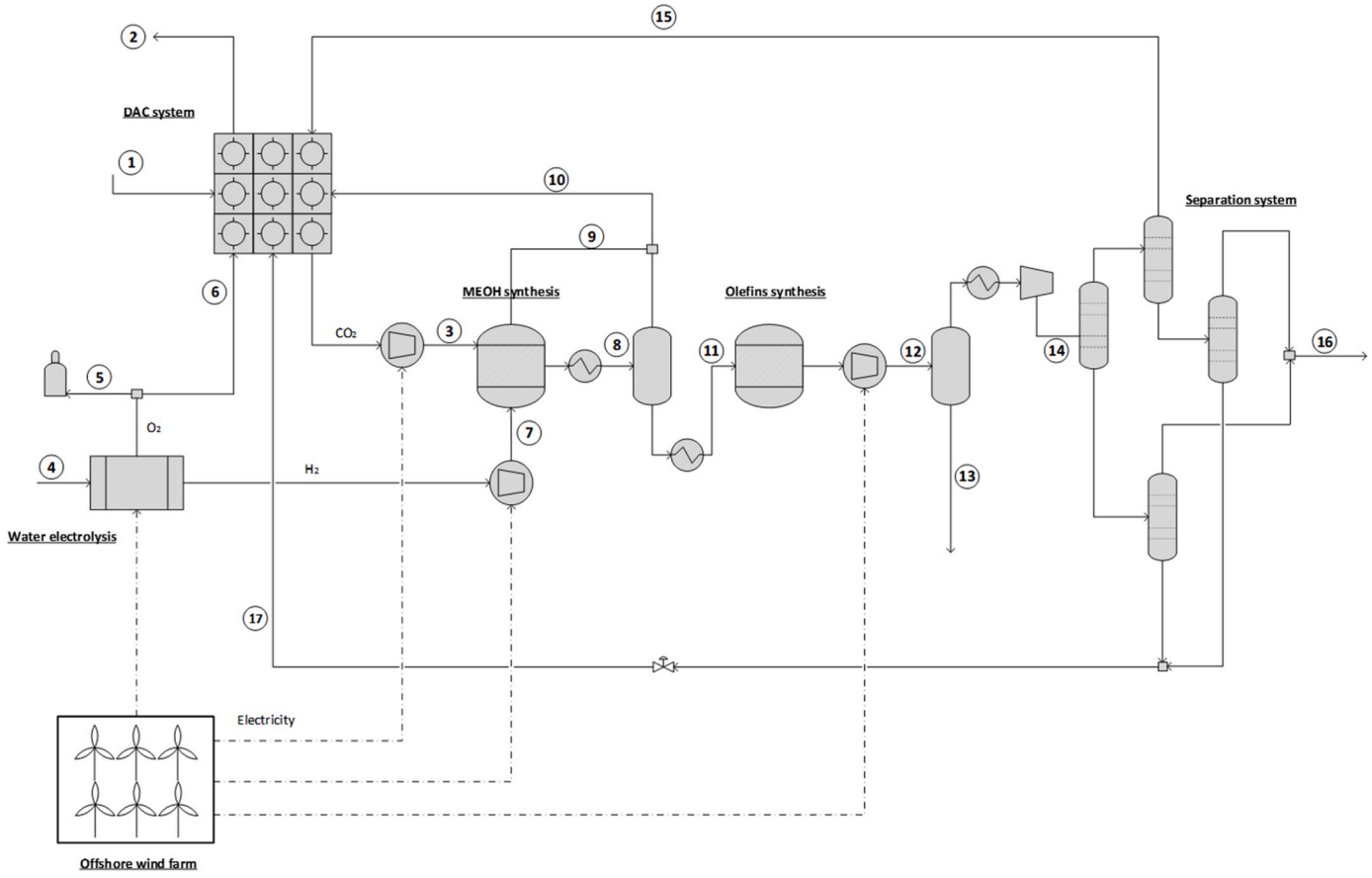

Fig. 7. Process Flow diagram and the main streams of the olefins production.

synthesis reactor. The stream containing the products was cooled down (stream 12) before the water removal (stream 13). Dehydrated olefins were compressed and further cooled (stream 14) before the column sequence. Heat was recovered and used to generate low pressure steam for the reboiler. Once in the separation section, light gases (stream 15) and the heavier C_4 and C_5 products (stream 17) are sent to the DAC oxy-fired combustion. Finally, ethylene and propylene are recovered as the main product (stream 16). Both achieved purities that are considered to be chemical grade (>95%) (Dow, 2022), about 98.7% and 98.2%, respectively. The CO_2 and H_2 to methanol per pass conversion in the methanol synthesis were 97.96% and 99.97%, respectively whereas an overall CO_2 conversion of 95.4% was achieved. A summary of the main inputs and outputs is shown in Table 5.

Further, Fig. 8 presents the exit mass fraction (dry basis) outputs of the olefins reactor and compares with experimental data derived from Lu et al. (2016). Clearly, the model obtained in this study is in good agreement with the experimental data with a slightly increment on the ethylene production. Also, the Coke content was compared to the results in the 5.31 g/100 g catalyst provided by the model against 5.64 g/100 g cat. reached in the experimental work.

4.1.1. Carbon balance

Fig. 9 displays the carbon flow through the PtO process. Initially, 1283 kmol/h of carbon enters the DAC and due to the capture efficiency part of the carbon is vented to the air (321 kmol/h). An additional carbon flow (449 kmol/h) is added to the system in the form of light gases coming from the MTO that are used in the calciner for energy recovery. Thus, the carbon exiting the DAC system is 1411 kmol/h and this is sent to the MTO and it is distributed into CH_3OH (methanol), CO_2, ethylene, propylene, butene (C_4), pentene (C_5), methane, propane and CO. A small amount of carbon is wasted in the methanol wastewater while the remaining carbon is partitioned between ethylene and propylene that leave the system as main products and the other olefin products that are used internally. The result of these carbon flow was an overall carbon efficiency of 72.3%, the major losses of carbon were in DAC due to the low capture efficiency (75%).

Do and Kim (2020), found a carbon efficiency of 99.2% of a CO_2 to

Table 5
Mass and energy inputs and outputs of the PtO.

Electrolyser		
Input	Amount	Unit
Electricity	526	MW
Deionised water	708	ktonne/y
Output		
H_2	76	ktonne/y
O_2	598	ktonne/y
Direct Air Capture		
Input		
Electricity	11.7	MW
Heat	67.2	MW
Output		
CO_2	554	ktonne/y
MTO plant		
Input		
CO_2	554	ktonne/y
H_2	76	ktonne/y
Electricity	19.3	MW
Output		
Olefins	103	ktonne/y
Light gases (CO, CH_4)	11.7	ktonne/y
C_{4+}	22.5	ktonne/y

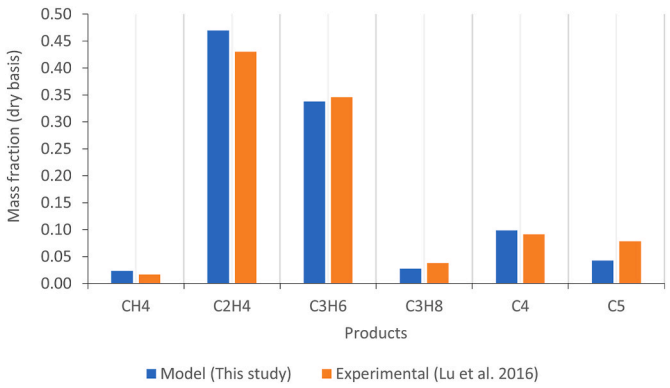

Fig. 8. Exit mass fraction composition (model) of the olefin reactor against experimental data from Lu et al. (2016).

C_2–C_4 process, which is higher than reported here. That is because our study includes the CO_2 capture, where most of the carbon is lost. The CO_2 capture is a crucial step of the infrastructure and must be included. Hence, the carbon efficiency can be improved by increasing the efficiency of the carbon capture technology. For example, CO_2 can be derived from biogenic sources (e.g., biomass or waste) or unavoidable point sources (e.g., cement plants) at capture rates greater than 90% by using typical amine-based post combustion processes. Further investigation on this aspect is highly recommended.

Based on the simulation, 4.88 tonne of CO_2 are required to produce 1 tonne of olefins. This lines up with Zhao et al. (2021) who estimated 4.3 tonne CO_2 per tonne of olefin. Do and Kim (2020) found that 1 tonne of C_2–C_4 hydrocarbons requires 3.89 tonne CO_2. Alternatively, since methanol production has been studied more than olefins, a comparison of the CO_2 to methanol ratio is also provided. From the present simulations, to produce 1 tonne of methanol, around 1.39 tonne of CO_2 is required. This has been compared to several studies (Arnaiz del Pozo et al., 2022; Bos et al., 2020; Nguyen and Zondervan, 2019; Sharma et al., 2022; Van-Dal and Bouallou, 2013a) in which the CO_2/MEOH ratio ranges between 1.56 and 1.69 tonne CO_2/tonne.

4.1.2. Energy balance

The electricity and heat requirements are the core of the PtO process. Table 6 shows the energy balance of the plant. The heat requirement in the DAC was around 67.2 MW (3.8 GJ/tonne CO_2) due to the thermal decomposition of carbonates in the calciner that requires high temperatures (900 °C). To supply this, three different streams were used to generate heat; the vented gases including H_2, CO and methanol in the MTO system, the off gases (CH_4, CO, CO_2, C_2H_4) and the heavier olefins C_{4+} recovered in the olefins purification section (stream 10, 15 and 17, in Fig. 7). Approximately 73.3 MW of heat was recovered by the oxy-combustion of these streams. The electricity consumption in the DAC was around 12 MW which was supplied by the steam turbine in the slaker. In the electrolyser, 526 MW of electricity was required due to the stack energy plus the auxiliary equipment. Also, the cooling energy was used to generate electricity in the ORC.

The MTO process had different energy requirements, heating was almost 107 MW while the cooling demand was 209 MW. Hot and cold streams in the MTO were integrated using a maximum temperature difference of 10 °C, resulting in a 100% and 47% covering, respectively for heating and cooling. Also, cooling remnant (110 MW) was used in the ORC, where 6.4 MW of electricity was generated. This amount was subtracted from the final PtO electricity demand resulted in 13 MW which was supplied by the offshore wind turbines.

The specific energy consumption reflects the energy consumption and the integration of the heat and cooling through the whole process per unit of product. It was found that PtO has an overall SEC of 150 MJ/kg olefin (41 kWh/kg). This includes the H_2 production through water electrolysis and CO_2 capture in addition to the olefin synthesis. The SEC is higher compared to the energy intensity of ethylene produced using different fossil - based feedstock such as ethane, naphtha and gas oil; these processes have a SEC that ranges between 19.4 and 31.9 MJ/kg (Worrell et al., 2000) and hence the PtO uses 5-fold more energy.

Table 6
Energy balance of the PtO process.

Unit/Process	Heat (kW)	Cooling (kW)	Electricity (kW)
DAC	67,281[a]	–	11,746[b]
Electrolyser	–	131,545[c]	526,299[d]
MTO	106,899[e]	208,979[e]	19,369[d]
Heat generation	77,344	–	–
Power generation (ORC)	–	–	6452

[a] Covered by heat generation.
[b] Covered by Steam turbine.
[c] Used in ORC power generation.
[d] Electricity covered by wind turbines.
[e] Heat Integrated.

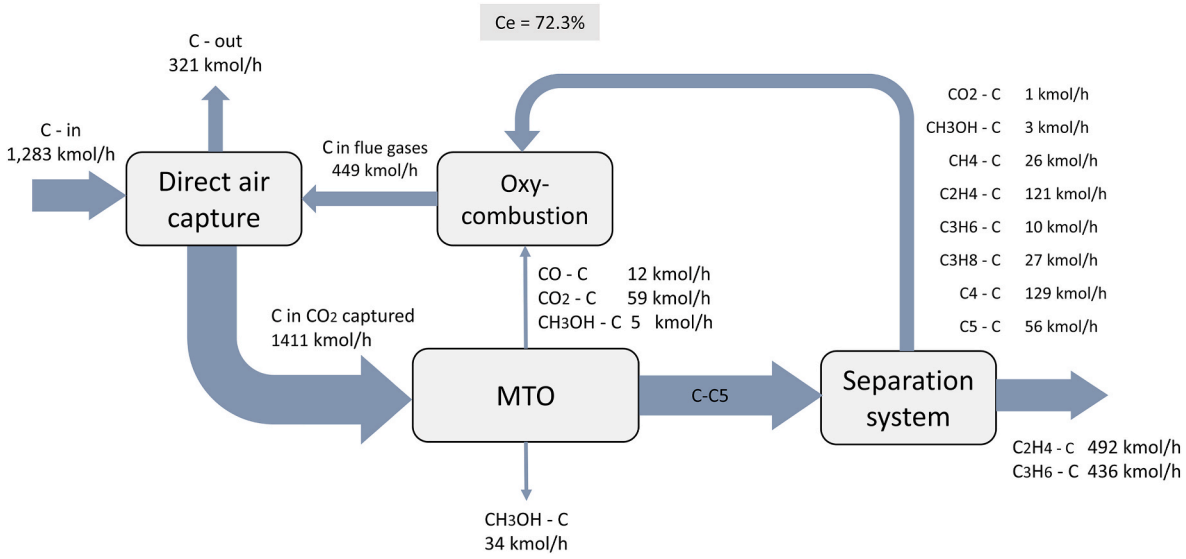

Fig. 9. Carbon flow in the proposed PtO process.

Compared to the PtX studies, Keller et al. (2020) reported a power demand of olefin from the CO_2 flue gases of about 96.9 MJ/kg olefins and this accounts for the electrolysis, flue gas scrubbing and olefin production. Further, the energy consumption in the PtX routes is intensive due to the high electricity consumption in the electrolyser.

All of the electricity of the plant was supplied by the off-shore wind farm. The wind farm had an arrangement of 176 Senvion turbines with a height of 87 m. They were able to provide around 540 MW of electricity with a capacity factor of 45.4% that indicates the average power output over the maximum power capability provided by the software. The power generated by the system clearly, is not constant, therefore, the fluctuations were covered by taking energy from grid, while the surplus energy was sent back to the grid to compensate for that consumption. Thus, the energy was in balance between the consumption and generation. The hourly power output of the farm is listed in the Supplementary information.

4.2. Economic analysis

In this study, the economic feasibility of the PtO process was assessed by estimating the olefins MSP. Table 7 presents the overall financial results. CAPEX included the PEC for the DAC, electrolyser, methanol, and olefins synthesis and separation. Around 825 million GBP are needed for the capital investment and 258 million GBP for the operational cost of the whole plant.

The breakdown of PEC is displayed in Fig. 10. As can be seen, the DAC contributes about 55% of the total purchased equipment cost, followed by the electrolyser with 37% and the olefin synthesis in 8%. As expected, the DAC implies a greater cost because the relative lack of technological development. The air contactor and the pellet reactor were the leading costs since they treat a large volume due to the low CO_2 concentration in the air (400 ppm). Within the water electrolysis, the costs include the stack, auxiliary equipment, and the additional compressors for the O_2 liquefaction. Lastly, MTO despite to list more equipment, it has a low contribution in the overall PEC.

Bos et al. (2020), evaluated the production of methanol through CO_2 hydrogenation using DAC and an alkaline electrolysis. They found that the cost of the CO_2 capture and the electrolysis dominate the PEC, accounting for 50% and 45%, respectively. As observed in Fig. 10, the DAC and H_2 production are the primary constraints in the fixed costs. It is expected that the costs of the capture decrease in the following years as the interest of its application at large scales increases, and more advanced technology is proved.

The operational cost distribution can be seen in Fig. 11. Clearly, the cost of the electricity is the dominant factor. It represents 85% of the total cost due to the large amount of electricity that is needed for the electrolyser in addition to the cost of the grid network usage that represents 17% within the cost. This finding is prevalent in the literature since it has been cited as being crucial in the economic viability in numerous research papers (Liu et al., 2020b; Nyári et al., 2020; Sharma et al., 2022; Shiva Kumar and Himabindu, 2019). The maintenance materials and labour, both composed, accounted for 9% of the total while insurances and tax contribute 3%. The catalysts, labour, and the rest of the expenses represented only about of 2% of the total.

The olefins MSP has been calculated through a break-even analysis.

Table 7
Economic CAPEX and OPEX results and the olefins MSP.

Parameter	Value	Units
CAPEX	£ 825	MMGBP
CAPEX/Unit	£ 7.98	£/kg
PEC	£ 277	MMGBP
FCI	£ 570	MMGBP
OPEX	£ 258	MMGBP
OPEX/unit	£ 2.49	£/kg

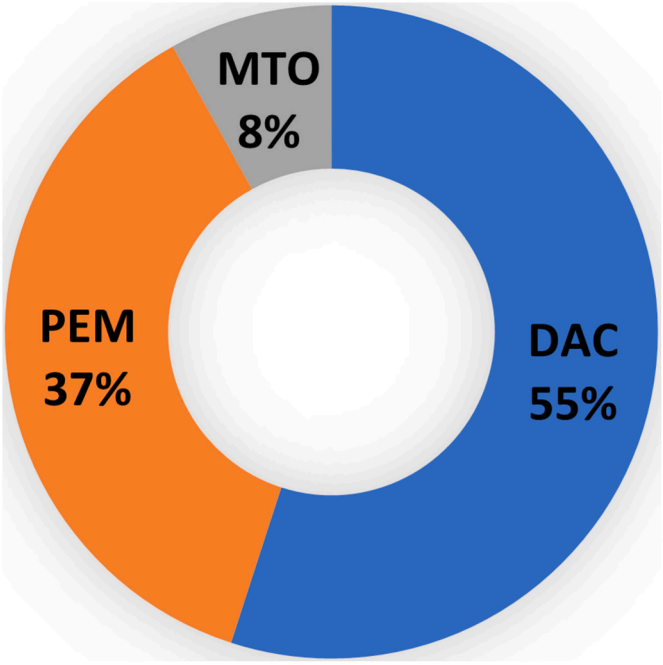

Fig. 10. Purchased equipment cost breakdown of the olefins plant.

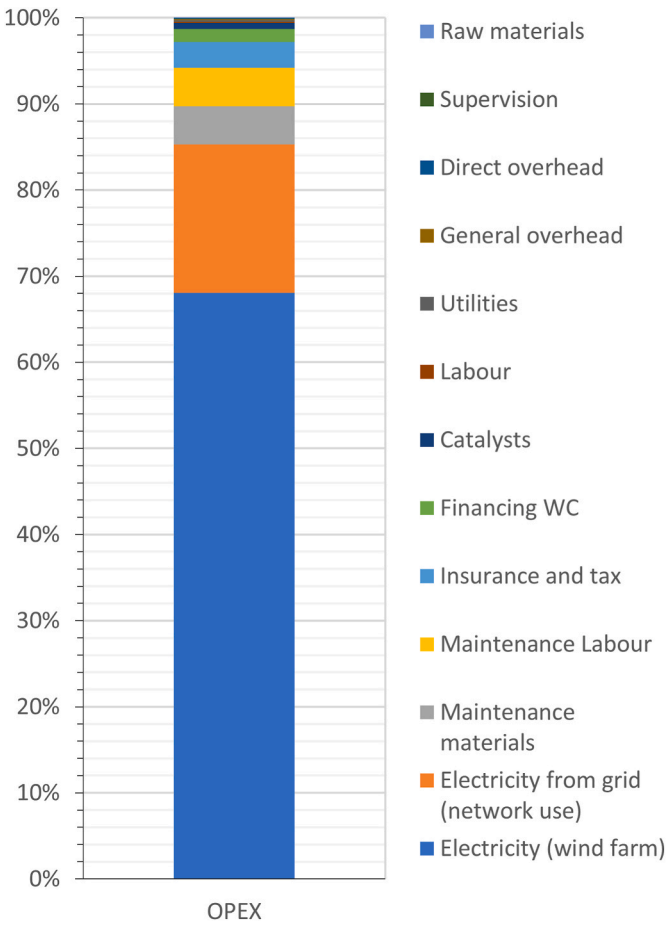

Fig. 11. Operational expenditures breakdown.

An estimated MSP of £3.67 per kg of olefin was resulted. The price is higher than the current market price for fossil - based ethylene and propylene production, which is around £1.05 – £1.4 per kg (Nyhus et al., 2024). Other studies have been evaluated olefins production in a Power to X approach with price ranging between £1.95 – £3.03 per kg olefins (Table 8) (Do and Kim, 2020; Goud et al., 2020; Pappijn et al., 2020; Savaete, 2016).

The range of prices primarily relies on the type of technology employed such as solar, wind, photovoltaic and nuclear renewable energy, and fossil-based options. Wind energy is one of the most profitable renewable electricity sources, however, the low electrolyser efficiency causes the effective energy utilisable is lower and more electricity must be supplied to meet the final request. Savaete (2016) estimated a price of £3.03/kg (€3.7/kg) olefin accounting for renewable methanol and stated by using fossil - based methanol feedstock, price drops to 0.93 €/kg. Do and Kim (2020) claimed a price of £2.79/kg C_2–C_4 product (USD 3.58/kg). They concluded that the use of fossil-fuel options for H_2 production result in relative low production cost but relative high emissions, in contrast, using renewable H_2 alternatives results in unfavourable economics for H_2 production highlighting the importance of a high efficiency electrolysis system.

The sensitivity analysis was performed to assess the influence of the parameters of interest over the olefins MSP. The LCOE, $LCCO_2$, electrolyser investment cost per MW, IRR and O_2 price were the considerations. The $LCCO_2$ was estimated as £150/tonne CO_2, which is in line with Keith et al. (2018), i.e. 94 to 232 USD/tonne CO_2; more details about the economic assumpions can be found in Keith et al. (2018). The sensitivity analysis result is represented in Fig. 12. As seen, the cost of the electricity leads to a notable effect on the olefins MSP. When the cost of electricity increases 25%, the MSP increases of about 12% over the original price (from £3.67 to £4.16). Conversely, if the LCOE decreases by 25%, the MSP reaches a value of £3.25, 12.6% less than the original price. Moreover, the CO_2 capture cost and the electrolyser investment cost had a moderate impact over the MSP, their variation was about half of the LCOE impact, about ±6% of the initial value. The IRR and the O_2 price showed minor impacts over the final price with changes below ±3% of the original price. Notably, improvements on the supply chain along with an effective utilisation of electricity should be further investigated to provide a better economic scenario for the PtX projects.

4.3. Life cycle assessment

In this paper, the Global Warming Potential impact is presented, discussed and compared. The results of the other impact categories can be consulted in the Supplementary material.

Table 8
Power to olefins economic results comparison.

Study	Main product	MSP[a], £/kg	Comments
Do and Kim (2020)	C_2–C_4 hydrocarbon	2.79	Onshore wind and electrolyser, CO_2 capture from MEA process.
Goud et al. (2020)	Ethylene	2.8	Purchased Methanol from renewables, MEA CO_2 captured
Goud et al. (2020)	Ethylene	2.1	H_2 from PEM using wind energy
Pappijn et al. (2020)	Ethylene	1.95	Electrochemical CO_2 conversion and wind energy
Savaete (2016)	Ethylene	3.03	Purchased renewable methanol
Nyhus et al. (2024)	Ethylene	2.92	Wind, DAC, AEL
Conventional olefin	Ethylene	1.05–104	Naphta, fossil-based energy
This study	Ethylene/ Propylene	3.67	Wind, PEM, DAC

[a] Prices in the original sources have been converted to GBP by using exchanges rates of the year.

The GWP emissions are expressed per FU, and only the process emissions were reported. The uptake of CO_2 entering the system during the capture and the end of life were excluded to preserve the carbon neutrality. This assumption was made in accordance with the study of Rosental et al. (2020). As a result of the adopted allocation in the electrolysis stage, all emissions were assigned to the H_2 because its exergy value was much higher than for O_2.

Table 9 shows the GWP impact breakdown of the PtO. About 0.74 kg CO_2e are emitted per kg olefin produced. In addition, the electrolysis stage is responsible for around 85% of the total emissions, with the remaining 15% being split between the DAC and the MTO stages.

The GWP of the electrolysis and MTO systems are dominated by the electricity consumption; despite the fact that wind electricity is employed, due to the high electricity consumption, predominantly in the electrolyser (a typical feature of Power-to-X systems), and the embedded emissions associated with the supply chains of the construction of the turbines the impact of electricity on the GWP is significant. Regarding the DAC, the necessary heat and electricity to run the system are covered internally; the H2-rich stream and the C4+ olefins stream from the MTO synthesis supplied heat while the electricity has been supplied by the steam turbine in the slaker (as described in thesupplementary information section A1.1). As a result, energy consumption has no contribution to the carbon emissions in the DAC system. Instead, emissions are caused by calcium and potassium additions, the water usage and waste disposal. The environmental impact breakdown of each stage is reported in the Supplementary Information.

To compare the PtO with the fossil - based process, a theoretical module of ethylene/propylene in the same proportions as in this study (47% and 53% respectively) from steam cracking of naphtha production, available in the Ecoinvent database v3.1 has been simulated in the Simapro software. The impact of this equivalent fossil - based olefin was 1.40 kg CO_2e per kg which is shown in Fig. 13. The results indicates that there is a 47% reduction in GWP by using PtO. This is because the fossil - based process is based on the use of fossil resources, such as the electricity from the grid which has a higher carbon intensity than the wind electricity.

The GWP value in the present study, i.e., 0.75 kg CO_2e/kg olefin, is similar to Rosental et al. (2020), who investigated the production of olefins through CO_2 that is captured using the *Climeworks* technology and an alkaline electrolytic H_2 in a cradle to the grave life cycle assessment including off-shore wind electricity. The global warming impact resulted for the olefins production was 0.76 kg CO_2e/kg (Fig. 13). Similar values of the GWP can be attributed to the fact that both studies used similar technologies, such as off-shore wind and DAC; the main difference is that Rosental et al. (2020) employs different technologies for H_2 and CO_2 production. In addition, they assume an electric-driven DAC while in the present study a complete energy integration has been applied. The heat requirement of the DAC has been covered internally by using the H2-rich stream and C4+ olefins from the MTO process. A steam turbine is employed in the DAC system to supply electrical need. Additionally, olefins have been used as refrigerants in an open loop in order to decrease the cooling need of the separation stage. Our design approach aims to efficiently integrate the different components of a Power-to-X system aiming at reducing costs and environmental impacts. This confirms that the low emissions in the PtX approaches are achievable and beneficial if renewable resources are combined with a total energy integration approach.

Based on a literature review, it was found that the GWP of olefins produced with CCU and electrolytic H_2, ranges between 0.37 and 2.6 kg CO_2e/kg olefin (Hoppe et al., 2018; Kuusela et al., 2021; Rosental et al., 2020) depending on the technology applied (Table 10), such as CO_2 capture from the biomass gasification, post combustion capture, or electrolytic CO_2 conversion in addition to the different technologies of H_2 production.

Another study performed by Keller et al. (2020) shows 14.01 kg CO_2e/kg olefin produced from secondary feedstock, such as flue gases

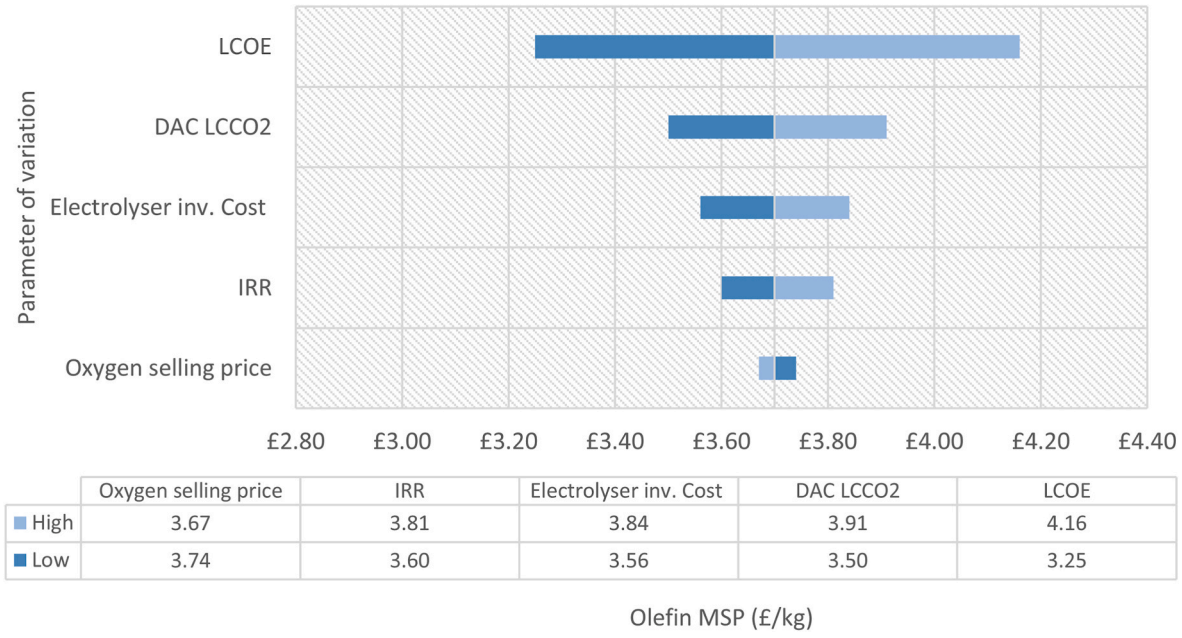

	Oxygen selling price	IRR	Electrolyser inv. Cost	DAC LCCO2	LCOE
High	3.67	3.81	3.84	3.91	4.16
Low	3.74	3.60	3.56	3.50	3.25

Fig. 12. Sensitivity analysis for the olefins MSP.

Table 9
Global warming potential impact of 1 kg of olefins.

Impact category	*Total*	Stage		
		DAC	*Electrolysis*	*MTO*
GWP (kg CO_2e/kg olefin)	0.74	0.08	0.64	0.02

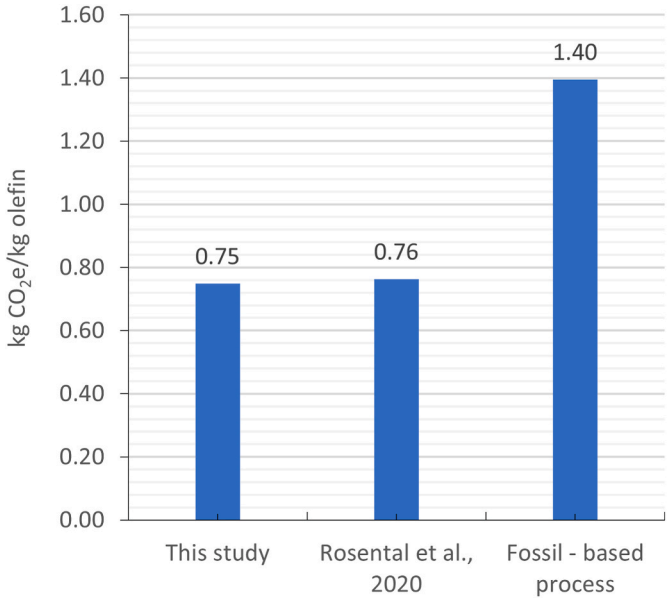

Fig. 13. Comparison of cradle to gate global warming potential of PtO with Rosental et al. (2020) and fossil - based process.

CO_2 extracted with amine-based scrubbing along with electrolytic H_2 powered by the grid and natural gas. They presented substitution electricity scenarios using wind turbines in which the GWP impact reached −1.77 kg CO_2e/kg olefin due to the inclusion of the CO_2 mitigation because of the uptake. When grid was substituted by wind the GWP drops to 2.2 kg CO_2e/kg olefin without accounting the uptake. They

Table 10
Global warming potential results comparison.

Study	FU (1 kg)	GWP, kg CO_2/kg FU	Comments
Rosental et al. (2020)	Ethylene	0.76	Wind, AEL, electrical DAC, accounting only processing emissions
Hoppe et al. (2018)	Polypropylene	2.3	DAC and wind energy for H_2 production, grid mix energy used in synthesis
Hoppe et al. (2018)	Polyethylene	2.5	DAC and wind energy for H_2 production, grid mix energy used in synthesis
Kuusela et al. (2021)	Polypropylene	2.6	CO_2 capture, electrolysis, methanol and propylene synthesis included.
Pappijn et al. (2020)	Ethylene	0.37	Wind, excluding CO_2 production and separation & purification stages
Keller et al. (2020)	Ethylene/ propylene	2.2	Flue gas, AEL electrolysis, wind energy
Conventional olefin	Ethylene	1.4	Naphta and fossil resources
This study	Ethylene/ propylene	0.74	DAC, wind energy for H_2 and synthesis, energy integration

came to the conclusion that the electricity supply is essential to use CO_2 feedstock and have positive environmental effects. The use of renewable resources, along with heat integration, improves the environmental performance of the PtX process and this has served as the motivation behind this research.

The electricity carbon intensity (CI) is a parameter of paramount importance in the environmental performance of PtX projects. The major drivers of the electricity CI are the construction materials of the fixed and moving parts of the turbines, which represent 48.9% and 49.8% of the total emissions, respectively (derived from Simapro). The CI of the wind electricity used in the PtO process was taken from the available module in the Simapro software for an offshore wind turbine in the United Kingdom. This module exhibits an emission factor of 0.0043 kg CO_2e/MJ of electricity (base case), however, according to the literature, it can vary between 0.002 and 0.123 depending on the size, model

and location of the turbines (Wang et al., 2019). Thus, a sensitivity analysis of the CI electricity on the GWP of the investigated process has been carried out. Fig. 14 displays the olefin GWP for a different wind electricity carbon intensity and the range of carbon intensity presented here varies from 0.002 to 0.01 kg CO_2e/MJ.

If the wind electricity CI reduces to 0.002 kg CO_2e/MJ, the GWP decreases by 42% and reaches a value 0.43 kg CO_2e/kg olefin. In contrast, when the base case CI is increased by 50% (from 0.0043 to 0.0086) the GWP increases by 44% up to 1.08 kg CO_2e/kg olefin.

The electricity from the current UK grid has a CI of 0.085 kg CO_2e/MJ. This means that the use of grid electricity is prohibitive for the investigated process as the GWP will rise to 12.96 kg CO_2e/kg olefin. This value is even much higher than the conventional ethylene/propylene production, thus demonstrating the importance of using renewable energies with low carbon intensities in PtX projects.

5. Conclusions

The paper focuses on a new and important detailed model for the power to olefin process employing direct air capture and electrolytic hydrogen from an offshore wind farm. Data on the economic and environmental performance of the power to olefins pathway are currently scarce. Current Power to olefins studies use system boundaries that typically exclude the CO_2 capture and/or the H_2 production, focusing on the olefins synthesis. In this paper a new and more comprehensive study of a cradle to gate power to olefins process considering also heat integration opportunities has been critically assessed to holistically assess the economic and environmental performance.

The PtO process has an overall carbon efficiency of 72.3%. Most of the carbon losses are in the DAC unit due to the CO_2 capture efficiency (i.e., 75%). Further, it is found that 4.64 kg of CO_2 is required to produce 1 kg olefin. The DAC heat requirement, i.e., 3.8 GJ/tonne CO_2, was covered internally after heat integration and hence no external source such as fossil fuel is required. Nevertheless, the specific energy consumption of the whole PtO assembly was higher than the respective fossil - based production due to the high electricity demand of the electrolyser, i.e. 150 MJ/kg vs 19.4–31.9 MJ/kg, respectively.

Based on a typical discounted cash flow analysis, the MSP of the PtO is more than three times higher than the market price of the conventional ethylene, i.e. 3.67 £/kg vs 1.05 £/kg, respectively. In addition, the sensitivity analysis exposed that the cost of electricity and the cost of CO_2 capture are the main cost drivers. A cradle-to-gate LCA estimated that the PtO process results in CO_2 emission reduction. The GWP drops by 47% compared to the fossil-based production. The dominant carbon emitter was the electrolysis, and it contributes around 85% of the process GWP. Further reductions of up to 69% can be achieved if the supply chains of wind energy further decarbonised.

Overall, the study assessed an integrated design for a low carbon olefins synthesis route contributing to the research of decarbonising the chemicals industry and the results can inform policy and engineering decision making.

CRediT authorship contribution statement

Gabriela A. Cuevas-Castillo: Conceptualization, Formal analysis, Investigation, Methodology, Software, Validation, Writing – original draft. **Stavros Michailos:** Conceptualization, Methodology, Software, Validation, Writing – review & editing. **Muhammad Akram:** Validation, Writing – review & editing. **Kevin Hughes:** Resources, Supervision, Writing – review & editing. **Derek Ingham:** Project administration, Resources, Supervision, Writing – review & editing. **Mohamed Pourkashanian:** Resources, Supervision, Writing – review & editing.

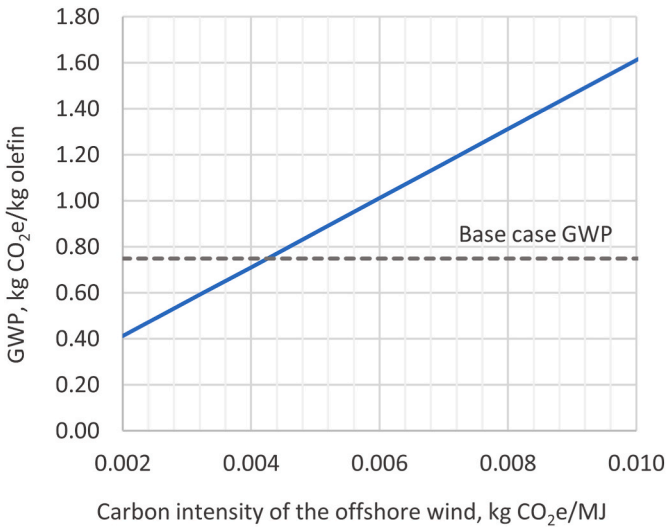

Fig. 14. Effect of the off-shore wind electricity carbon intensity on the olefin GWP (dashed line indicates base case olefin GWP).

Declaration of competing interest

The authors declare that they have no known competing financial interests or personal relationships that could have appeared to influence the work reported in this paper.

Data availability

Data will be made available on request.

Acknowledgements

The first author is grateful to the Mexican Council for Science and Technology (CONACYT) for the PhD scholarship (cvu 703759). The second author is grateful to the R and I Support Fund provided by University of Hull.

Appendix A. Supplementary data

Supplementary data to this article can be found online at https://doi.org/10.1016/j.jclepro.2024.143143.

References

Alonso-Fariñas, B., Gallego-Schmid, A., Haro, P., Azapagic, A., 2018. Environmental assessment of thermo-chemical processes for bio-ethylene production in comparison with bio-chemical and fossil-based ethylene. J. Clean. Prod. 202, 817–829. https://doi.org/10.1016/j.jclepro.2018.08.147.

Althaus, H., Chudacoff, M., Hischier, R., Jungbluth, N., Osses, M., Primas, A., Hellweg, S., 2007. Life Cycle Inventories of Chemicals. Ecoinvent Report No.8, v2.0. Final Rep. Ecoinvent Data, pp. 1–957.

Arnaiz del Pozo, C., Cloete, S., Jiménez Álvaro, Á., 2022. Techno-economic assessment of long-term methanol production from natural gas and renewables. Energy Convers. Manag. 266 https://doi.org/10.1016/j.enconman.2022.115785.

Bianchi, S., 2020. Process Modelling of a Direct Air Capture (DAC) System Based on the Kraft Process 100.

Bos, M.J., Kersten, S.R.A., Brilman, D.W.F., 2020. Wind power to methanol: renewable methanol production using electricity, electrolysis of water and CO2 air capture. Appl. Energy 264, 114672. https://doi.org/10.1016/j.apenergy.2020.114672.

Buttler, A., Spliethoff, H., 2018. Current status of water electrolysis for energy storage, grid balancing and sector coupling via power-to-gas and power-to-liquids: a review. Renew. Sustain. Energy Rev. 82, 2440–2454. https://doi.org/10.1016/j.rser.2017.09.003.

Chung, C., Kim, J., Sovacool, B.K., Bazilian, M., Griffiths, S., Yang, M., 2023. Decarbonizing chemical industry: a systematic review of sociotechnical systems, technological innovations, and policy options. Energy Res. Social Sci. 89, 102955 https://doi.org/10.1016/j.erss.2022.102565.

Do, T.N., Kim, J., 2020. Green C2-C4 hydrocarbon production through direct CO2 hydrogenation with renewable hydrogen: process development and techno-

economic analysis. Energy Convers. Manag. 214, 112866 https://doi.org/10.1016/j.enconman.2020.112866.
Dow, 2022. Ethylene [WWW document]. URL. https://www.dow.com/en-us/pdp.ethylene.31681z.html#overview.
Dutta, A., Karimi, I.A., Farooq, S., 2019. Technoeconomic perspective on natural gas liquids and methanol as potential feedstocks for producing olefins. Ind. Eng. Chem. Res. 58, 963–972. https://doi.org/10.1021/acs.iecr.8b05277.
Ekvall, T., Tillman, A.M., 1997. Open-loop recycling: criteria for allocation procedures. Int. J. Life Cycle Assess. 2, 155–162. https://doi.org/10.1007/BF02978810.
Eurostat, 2021. Eurostat database [WWW Document]. URL. https://ec.europa.eu/eurostat/web/main/eurostat/web/main/help/faq/data-services.
Fasihi, M., Efimova, O., Breyer, C., 2019. Techno-economic assessment of CO 2 direct air capture plants. J. Clean. Prod. 224, 957–980. https://doi.org/10.1016/j.jclepro.2019.03.086.
Fernanda Rojas Michaga, M., Michailos, S., Akram, M., Cardozo, E., Hughes, K.J., Ingham, D., Pourkashanian, M., 2022. Bioenergy with carbon capture and storage (BECCS) potential in jet fuel production from forestry residues: a combined Techno-Economic and Life Cycle Assessment approach. Energy Convers. Manag. 255, 115346 https://doi.org/10.1016/j.enconman.2022.115346.
Finkbeiner, M., Bach, V., 2021. Life Cycle Assessment of Decarbonization Options-Towards Scientifically Robust Carbon Neutrality, vol. 26, pp. 635–639. https://doi.org/10.1007/s11367-021-01902-4.
Fontalvo, J., 2014. Usando modelos de usuario en Matlab en la interfaz de Aspen plus con Excel como puente. Ing. Invest. 34, 39–43.
Garcia-Garcia, G., Fernandez, M.C., Armstrong, K., Woolas, S., Styring, P., 2021. Analytical review of life-cycle environmental impacts of carbon capture and utilization technologies. Chem. Sustain. Energy Mater. 14, 995–1015.
Goud, D., Gupta, R., Maligal-ganesh, R., Peter, S.C., 2020. Review of catalyst design and mechanistic studies for the production of ole fi ns from anthropogenic CO 2. https://doi.org/10.1021/acscatal.0c03799.
GPCA, 2019. Ethylene: a litmus test for the chemical industry. Gulf Petrochemicals Chem. Assoc. 8.
Hank, C., Gelpke, S., Schnabl, A., White, R.J., Full, J., Wiebe, N., Smolinka, T., Schaadt, A., Henning, H.M., Hebling, C., 2018. Economics & carbon dioxide avoidance cost of methanol production based on renewable hydrogen and recycled carbon dioxide-power-to-methanol. Sustain. Energy Fuels 2, 1244–1261. https://doi.org/10.1039/c8se00032h.
Harrison, K.W., Remick, R., Martin, G.D., 2014. Hydrogen production: fundamentals and case study summaries. Natl. Renew. Energy Lab. 2, 6–11.
Herz, G., Rix, C., Jacobasch, E., Müller, N., Reichelt, E., Jahn, M., Michaelis, A., 2021. Economic assessment of Power-to-Liquid processes – influence of electrolysis technology and operating conditions. Appl. Energy 292. https://doi.org/10.1016/j.apenergy.2021.116655.
Hoppe, W., Thonemann, N., Bringezu, S., 2018. Life cycle assessment of carbon dioxide–based production of methane and methanol and derived polymers. J. Ind. Ecol. 22, 327–340. https://doi.org/10.1111/jiec.12583.
IEA, 2018. The future of petrochemicals. Futur. petrochemicals. https://doi.org/10.1787/9789264307414-en.
IEA, 2019. Transforming Industry through CCUS.
Jiang, P., Parvez, A.M., Meng, Y., Xu, M. xia, Shui, T. chi, Sun, C. gong, Wu, T., 2019. Exergetic, economic and carbon emission studies of bio-olefin production via indirect steam gasification process. Energy 187. https://doi.org/10.1016/j.energy.2019.115933.
Johnson, W.L., Hauser, D.M., Plachta, D.W., Wang, X.Y.J., Banker, B.F., Desai, P.S., Stephens, J.R., Swanger, A.M., 2018. Comparison of oxygen liquefaction methods for use on the Martian surface. Cryogenics (Guildf) 90, 60–69. https://doi.org/10.1016/j.cryogenics.2017.12.008.
Keith, D.W., Holmes, G., St Angelo, D., Heidel, K., 2018. A process for capturing CO2 from the atmosphere. Joule 2, 1573–1594. https://doi.org/10.1016/j.joule.2018.05.006.
Keller, F., Lee, R.P., Meyer, B., 2020. Life cycle assessment of global warming potential, resource depletion and acidification potential of fossil, renewable and secondary feedstock for olefin production in Germany. J. Clean. Prod. 250, 119484 https://doi.org/10.1016/j.jclepro.2019.119484.
Kibria Nabil, S., McCoy, S., Kibria, M.G., 2021. Comparative life cycle assessment of electrochemical upgrading of CO2to fuels and feedstocks. Green Chem. 23, 867–880. https://doi.org/10.1039/d0gc02831b.
Knighton, L.T., Snowden-Swan, L., Wendt, D.S., Jenks, J., Askander, J., Li, S., 2020. Techno-economic analysis of synthetic fuels pathways integrated with light water reactors. U.S. Dep. Energy.
Kuusela, K., Uusitalo, V., Ahola, J., 2021. The transformation of plastics production from net positive greenhouse gas emissions to net negative : an environmental sustainability assessment of CO 2 -based polypropylene 52. https://doi.org/10.1016/j.jcou.2021.101672.
Liu, C.M., Sandhu, N.K., McCoy, S.T., Bergerson, J.A., 2020a. A life cycle assessment of greenhouse gas emissions from direct air capture and Fischer-Tropsch fuel production. Sustain. Energy Fuels 4, 3129–3142. https://doi.org/10.1039/c9se00479c.
Liu, C.M., Sandhu, N.K., McCoy, S.T., Bergerson, J.A., 2020b. A life cycle assessment of greenhouse gas emissions from direct air capture and Fischer-Tropsch fuel production. Sustain. Energy Fuels 4, 3129–3142. https://doi.org/10.1039/c9se00479c.
Lu, B., Luo, H., Li, H., Wang, W., Ye, M., Liu, Z., Li, J., 2016. Speeding up CFD simulation of fluidized bed reactor for MTO by coupling CRE model. Chem. Eng. Sci. 143, 341–350. https://doi.org/10.1016/j.ces.2016.01.010.
Lundberg, S., 2019. Comparative LCA of Electrolyzers for Hydrogen Gas Production 99.
Manwell, J.F., McGowan, J.G., Rogers, A.L., 2010. Wind Energy Explained: Theory, Design and Application. John Wiley & Sons, Inc.
McQueen, N., Psarras, P., Pilorgé, H., Liguori, S., He, J., Yuan, M., Woodall, C.M., Kian, K., Pierpoint, L., Jurewicz, J., Lucas, J.M., Jacobson, R., Deich, N., Wilcox, J., 2020. Cost analysis of direct air capture and sequestration coupled to low-carbon thermal energy in the United States. Environ. Sci. Technol. 54, 7542–7551. https://doi.org/10.1021/acs.est.0c00476.
Meteotest, 2020. Meteonorm version 8 [WWW Document]. URL. https://meteonorm.meteotest.ch/en/, 10.29.22.
Michailos, S., McCord, S., Sick, V., Stokes, G., Styring, P., 2019. Dimethyl ether synthesis via captured CO2 hydrogenation within the power to liquids concept: a techno-economic assessment. Energy Convers. Manag. 184, 262–276. https://doi.org/10.1016/j.enconman.2019.01.046.
Mignard, D., Pritchard, C., 2008. On the use of electrolytic hydrogen from variable renewable energies for the enhanced conversion of biomass to fuels. Chem. Eng. Res. Des. 86, 473–487. https://doi.org/10.1016/j.cherd.2007.12.008.
Mohsenzadeh, A., Zamani, A., Taherzadeh, M., 2017. Bioethylene production from ethanol A review and techno-economical evaluation. Chem. Bioeng. 4, 3. https://doi.org/10.1002/cben.201600025.
Mostafa, M., Antonicelli, C., Varela, C., Barletta, D., Zondervan, E., 2022. Capturing CO2 from the atmosphere: design and analysis of a large-scale DAC facility. Carbon Capture Sci. Technol. 4, 100060 https://doi.org/10.1016/j.ccst.2022.100060.
Nguyen, T.B.H., Zondervan, E., 2019. Methanol production from captured CO2 using hydrogenation and reforming technologies- environmental and economic evaluation. J. CO2 Util. 34, 1–11. https://doi.org/10.1016/j.jcou.2019.05.033.
Nyári, J., Magdeldin, M., Larmi, M., Järvinen, M., Santasalo-Aarnio, A., 2020. Techno-economic barriers of an industrial-scale methanol CCU-plant. J. CO2 Util. 39 https://doi.org/10.1016/j.jcou.2020.101166.
Nyhus, A.H., Yliruka, M., Shah, N., Chachuat, B., 2024. Green ethylene production in the UK by 2035: a techno-economic assessment. Energy Environ. Sci. 17, 1931–1949. https://doi.org/10.1039/d3ee03064d.
Obrist, M.D., Kannan, R., Schmidt, T.J., Kober, T., 2021. Decarbonization pathways of the Swiss cement industry towards net zero emissions. J. Clean. Prod. 288 https://doi.org/10.1016/j.jclepro.2020.125413.
Office for National Statistics, 2020. A01: summary of labour market statistics [WWW Document]. Off. Natl. Stat. URL. https://www.ons.gov.uk/employmentandlabourmarke%0At/peopleinwork/employmentandemployeetypes/datasets/summaryoflabourmar%0Aketstatistics.
Pappijn, C.A.R., Ruitenbeek, M., Reyniers, M.F., Van Geem, K.M., 2020. Challenges and opportunities of carbon capture and utilization: electrochemical conversion of CO2 to ethylene. Front. Earth Sci. 8, 1–12. https://doi.org/10.3389/fenrg.2020.557466.
Pérez-Fortes, M., Bocin-Dumitriu, A., Tzimas, E., 2014. CO2 utilization pathways: techno-economic assessment and market opportunities. In: Energy Procedia. Elsevier Ltd, pp. 7968–7975. https://doi.org/10.1016/j.egypro.2014.11.834.
Pérez-Fortes, M., Schöneberger, J.C., Boulamanti, A., Tzimas, E., 2016. Methanol synthesis using captured CO2 as raw material: techno-economic and environmental assessment. Appl. Energy 161, 718–732. https://doi.org/10.1016/j.apenergy.2015.07.067.
Peters, M.S., Timmerhaus, K.D., 2002. Plant Design and Economics for Chemical Engineers, fifth ed. McGraw-Hill, Estados Unidos.
Peters, R., Baltruweit, M., Grube, T., Samsun, R.C., Stolten, D., 2019. A techno economic analysis of the power to gas route. J. CO2 Util. 34, 616–634. https://doi.org/10.1016/j.jcou.2019.07.009.
Prats-Salvado, E., Monnerie, N., Sattler, C., 2022. Techno-economic assessment of the integration of direct air capture and the production of solar fuels. Energies 15. https://doi.org/10.3390/en15145017.
Rosental, M., Fröhlich, T., Liebich, A., 2020. Life cycle assessment of carbon capture and utilization for the production of large volume organic chemicals. Front. Clim. 2, 1–14. https://doi.org/10.3389/fclim.2020.586199.
Sabatino, F., Gazzani, M., Grimm, A., Gallucci, F., Van Sint Annaland, M., Kramer, G.J., 2018. Comparative assessment and optimization of direct air capture via absorption and adsorption processes. Int. Conf. Negat. CO2 Emiss. 22–24, 2018, Göteborg, Sweden 2018.
Sabatino, F., Grimm, A., Gallucci, F., van Sint Annaland, M., Kramer, G.J., Gazzani, M., 2021. A comparative energy and costs assessment and optimization for direct air capture technologies. Joule 5, 2047–2076. https://doi.org/10.1016/j.joule.2021.05.023.
Salkuyeh, Y.K., Adams, T.A., 2015. Co-production of olefins, fuels, and electricity from conventional pipeline gas and shale gas with near-zero CO2 emissions. Part I: process development and technical performance. Energies 8, 3739–3761. https://doi.org/10.3390/en8053739.
Sanz-Pérez, E.S., Murdock, C.R., Didas, S.A., Jones, C.W., 2016. Direct capture of CO2 from ambient air. Chem. Rev. https://doi.org/10.1021/acs.chemrev.6b00173.
Savaete, T., 2016. Catalytic CO 2 Conversion : a Techno-Economic Analysis and Theoretical Study.
Sharma, I., Shah, V., Shah, M., 2022. A comprehensive study on production of methanol from wind energy. Environ. Technol. Innov. 28, 102589 https://doi.org/10.1016/j.eti.2022.102589.
Shiva Kumar, S., Himabindu, V., 2019. Hydrogen production by PEM water electrolysis – a review. Mater. Sci. Energy Technol. 2 https://doi.org/10.1016/j.mset.2019.03.002.
Towler, G., Sinnott, R., 2008. Chemical Engineering Design: Principles, Practice and Economics of Plant and Process Design. United States Am. Elvesier Inc.
Van-Dal, É.S., Bouallou, C., 2013a. Design and simulation of a methanol production plant from CO2 hydrogenation. J. Clean. Prod. 57, 38–45. https://doi.org/10.1016/j.jclepro.2013.06.008.

Van-Dal, É.S., Bouallou, C., 2013b. Design and simulation of a methanol production plant from CO2 hydrogenation. J. Clean. Prod. 57, 38–45. https://doi.org/10.1016/j.jclepro.2013.06.008.

Vanden Bussche, K.M., Froment, G.F., 1996. A steady-state kinetic model for methanol synthesis and the water gas shift reaction on a commercial Cu/ZnO/Al2O3 catalyst. J. Catal. 161, 1–10. https://doi.org/10.1006/jcat.1996.0156.

Wang, S., Wang, S., Liu, J., 2019. Life-cycle green-house gas emissions of onshore and offshore wind turbines. J. Clean. Prod. 210, 804–810. https://doi.org/10.1016/j.jclepro.2018.11.031.

DE-AC03-76SF00098 Worrell, E., Ernst, Worrell, Phylipsen, D., Einstein, D., Martin, N., 2000. Energy Use and Energy Intensity of the US. Chem. Ind. Energy Anal. Dep. Environ.. https://doi.org/10.2172/773773.

Xiang, D., Yang, S., Li, X., Qian, Y., 2015. Life cycle assessment of energy consumption and GHG emissions of olefins production from alternative resources in China. Energy Convers. Manag. 90, 12–20. https://doi.org/10.1016/j.enconman.2014.11.007.

Yang, M., You, F., 2017. Comparative techno-economic and environmental analysis of ethylene and propylene manufacturing from wet shale gas and naphtha. Ind. Eng. Chem. Res. 56, 4038–4051. https://doi.org/10.1021/acs.iecr.7b00354.

Zhao, Z., Jiang, J., Wang, F., 2021. An economic analysis of twenty light olefin production pathways. J. Energy Chem. 56, 193–202. https://doi.org/10.1016/j.jechem.2020.04.021.